Vacancy-oxygen defects in silicon: the impact of isovalent doping

Londos, C.A. , Sgourou, E.N. , Hall, D. and Chroneos, A.

Original citation:
Londos, C.A. , Sgourou, E.N. , Hall, D. and Chroneos, A. (2014) Vacancy-oxygen defects in silicon: the impact of isovalent doping. Journal of Materials Science: Materials in Electronics, volume 25 (6): 2395-2410. DOI: 10.1007/s10854-014-1947-6

http://dx.doi.org/10.1007/s10854-014-1947-6

Springer US

The final publication is available at Springer via http://dx.doi.org/10.1007/s10854-014-1947-6

REVIEW

Vacancy-oxygen defects in silicon: the impact of isovalent doping

C. A. Londos,[1] E. N. Sgourou,[1] D. Hall,[2] A. Chroneos[3,4]

[1]*Solid State Section, Physics Department, University of Athens, Panepistimiopolis, Zografos, 157 84 Athens, Greece*
[2]*Department of Physical Sciences, The Open University, Milton Keynes MK7 6AA, United Kingdom*
[3]*Engineering and Innovation, The Open University, Milton Keynes MK7 6AA, United Kingdom*
[4]*Department of Materials, Imperial College London, London SW7 2BP, United Kingdom*

Abstract

Silicon is the mainstream material for many nanoelectronic and photovoltaic applications. The understanding of oxygen related defects at a fundamental level is essential to further improve devices, as vacancy-oxygen defects can have a negative impact on the properties of silicon. In the present review we mainly focus on the influence of isovalent doping on the properties of A-centers in silicon. Wherever possible, we make comparisons with related materials such as silicon germanium alloys and germanium. Recent advanced density functional theory studies that provide further insights on the charge state of the A-centers and the impact of isovalent doping are also discussed in detail.

1. Introduction

Silicon (Si) pervades modern society in a number of ways due to its seemingly endless number of applications aiming to improve the quality of our lives. The advantageous properties of Si in comparison with other electronic materials have made it the basic building block for the electronic industry for numerous years. However, Si is not perfect and contains defects in the lattice which can act to deteriorate the performance of the devices. To improve Si devices and allow incorporation into new applications it is necessary to explore the properties and behaviour from a fundamental viewpoint.

The introduction of defects in semiconductors is unavoidable in common device processing, for example by radiation, implantations, diffusion, contamination with impurities and through material processing. Knowledge about the properties and the behaviour of defects, and especially regarding the fundamental processes and reactions in which they participate, are essential for understanding various technological problems related to, for example, limitations in fabrication. Furthermore issues related to the operation of the devices in specific environments, such as in accelerators where radiation damage can deteriorate their functionality, could be more easily overcome if we knew more about the properties of the defects present.

Intrinsic defects, namely vacancies and self-interstitials, are known to play a fundamental role in many solid state processes such as diffusion, strain release in the lattice or radiation effects. In the latter case, the formation of various radiation-induced defects is the result of direct or indirect participation of intrinsic defects and various impurities in the material. One way to study these defects in a controlled manner is through the exposure of the material to high energy particles such as electrons, neutrons, protons or gamma-rays. In Si, both vacancies (*V*) and self-

interstitials (Si_I) are highly mobile and can form pairs and/or complexes with other impurities and other intrinsic defects present in the lattice, such as in the example of vacancies that can be readily captured by oxygen to form *V*O pairs. Thus, by studying the properties of the latter mentioned centre, valuable information can be retrieved regarding the vacancies.

One vitally important issue with respect to wafer fabrication and device processing is the control of induced defects in order to prevent device degradation and to aid in the development of new methods for avoiding these defects by design. Vacancies, along with self-interstitials, are intrinsic defects in Si and the primary defects produced by irradiation [1]; they are the building blocks participating directly or indirectly in the formation of radiation defects in Si. *V*O formation itself involves an interaction with the vacancy. Subsequently, any information acquired about the production and the properties of the *V*O defect would certainly serve to improve our understanding on the role of vacancies in many other processes in Si.

The *V*O defect in Si is an electrically active centre, introducing an energy level within the semiconductor gap, reported at E_c-0.17 eV [2]. It is an important recombination centre in Si providing a channel for charge carriers, thus it consequently affects the electrical properties of Si. Generally, the *V*O defect has an adverse effect on the performance of the device in consideration [3]. Notably, efficient intercentre charge transfer has been reported between the deep *V*O (-/0) level at (E_c-0.17 eV) and the shallow phosphorus substitutional donor level at E_c-0.045 eV [4] as well as between the $(C_iO_i)^o$ defect in its excited state and the $(V\text{-}O)^o$ [5].

C_iO_i is another important recombination centre in Si [6]. The phenomenon of communication between defects is very important in understanding the mechanisms of trapping and recombination of non equilibrium charge carriers at defect levels.

Investigations have led to conclusions that the A-centre may be amphoteric, and besides the neutral and the negative charge state, a positive charge state may exist alongside additional levels in the gap [5,7,8]. It has also been implied [9] that the *V*O defect is a negative–U centre with single donor state (0/+) deep in the valence band, which is the reason that the level has not yet been detected. It has been suggested that the centre contains all the physics of metastability, although this phenomenon cannot be manifested due to the fact that the effect is too strong. Clearly, a full picture on the issue will provide further means with which to suppress the negative effects of defects that show recombination activity.

Measurements of oxygen diffusion and oxygen aggregation processes in Si have undoubtedly shown an enhanced oxygen diffusion [10]. Several models have been suggested to interpret the phenomenon. Thus, the observed enhanced diffusion of oxygen in Si has been attributed to interactions of O_i atoms with lattice vacancies [11,12], with self-interstitials [13], with metallic contaminants (for example copper, iron etc) [14] or non-metallic elements such as carbon [15], hydrogen [16], nitrogen [17] or isovalent dopants as Ge, Sn, Pb [18-20] or even with a second oxygen leading to fast diffusing oxygen dimers [21].

In particular, *V*O has also been proposed to act as a vehicle to enhance oxygen diffusion [11,12]. It has been suggested that the formation and rapid dissociation of *V*O centres could play a role and may account for the enhanced oxygen diffusion in heat-treated Si by reducing the barrier of oxygen diffusion jumps in the Si lattice. Monte Carlo simulations [22] show that oxygen impurities influence the aggregation of voids during crystal growth conditions via the formation of oxygen-vacancy complexes [23].

Upon thermal annealing, *V*O is converted to various V_nO_m defects by the addition of vacancies and/or oxygen atoms in the initial *V*O core. **i)** V_nO_m complexes cause leakage currents in *p*-*n* junctions [24-26]. Also besides *V*O, the V_2O and V_3O defects have been found to be effective recombination centers contributing in the reduction of the minority charge carriers lifetime induced by irradiation [3,27]. **ii)** It has also been assumed that large VO_n (n = 4, 5, 6) complexes enhance oxygen precipitation in irradiated Si, most probably acting as heterogeneous nuclei of oxygen precipitates [28-31]. In essence, VO_n provide additional nuclei for oxygen precipitation. Upon annealing *V*O is converted to VO_2 by the addition of an oxygen atom. Theoretical calculations have concluded that some kind of *V*O and VO_2 complexes could exist at temperatures of up to 1200 ^oC and affect oxygen aggregation processes in Si [32-34]. In this framework, VO_2 defects have been suggested to play an important role as a nucleation centre in the formation of oxygen precipitation in un-irradiated Si [32].

In order to control radiation defects in semiconductors, a model of the effects of radiation damage is required. The key to qualifying and quantifying this damage is an in depth understanding of the properties and the behaviour of radiation induced defects. In other words, predictive modelling of radiation damage in electronic devices requires not only a detailed quantitative, but also a qualitative, understanding of the behaviour of the fundamental defects in the device material.

Si, as with any other crystal, is inherently imperfect and contains defects. Besides vacancies and self-interstitials that are created by thermodynamic processes, other impurities and complexes can be introduced to the lattice during crystal growth and material processing, dramatically altering the properties of the material. For instance, the controlled addition of *p*- or *n*-type dopants in Si, even by just one atom

per million Si host atoms, could significantly affect the electronic properties of the material. This represents the positive side of doping and it was the first giant step which led, in essence, to the electronic era and the foundation of the semiconductor industry. Central to this, the control of the properties and behaviour of the defects incorporated in the material is one of the most important issues in Si-based technology, and also more generally within semiconductors. This is the so-called defect engineering strategy, aiming to control the introduction and/or suppression of defects produced during crystal growth and processing for device fabrication in order to enhance the quality of the material for certain applications. Also, to reduce any limited factors for a further increase in the efficiency of devices and to expand the material's applicability in new areas of the respective industry. This is particularly important for Si, since the continuous downscaling of the device magnitude has now reached the limits of the Si material and there is therefore an urgent need to explore new ways that could further extend these limits to meet the demands of new electronic applications.

The present review is focused on vacancy-oxygen defects and their interaction with isovalent atoms. The first part concerns the motivation for studying A-centres in view of a recent technological example. This is followed by a review of the *V*O and VO_2 defects from an experimental and density functional theory perspective. The third and main part concerns the impact of isovalent doping, the trends observed, the perspectives and potential defect engineering strategies. Finally, a brief summary and future directions are given.

2. Motivation

Silicon has been a material of choice for imaging and spectroscopy detectors for many years. The presence of defects in the silicon lattice has, however, often caused problems in the application for which the sensor is being used. Si-based detectors operate through the collection and readout of charge, generated through the photo-electric effect from incident photons (whether visible or X-ray). However, there are other sources of charge within the device, including those generated by defects in the Si lattice. This "extra" signal can give rise to several effects, including Random Telegraph Signals or increased dark current [35,36]. In the case of a *n*-channel Charge-Coupled Device (CCD) the signal electrons must also be transferred through the device before readout. As the electrons pass through the silicon of the device they can encounter defects, or "traps", which act to capture electrons from the charge packet, later emitting these into following packets, causing a smearing of the image and reducing the efficiency of the charge transfer mechanism, as shown in Figure 1 (left), [37].

Charge-Coupled Devices have been the detector of choice for use in the focal plane of many space missions. When in space, the harsh radiation environment causes the creation of many defects or "traps" in Si. For example, when a high energy proton passes into the detector, not only can the ionising trail cause an increase in oxide charge and surface dark current [35], but the proton can cause displacement damage, effectively knocking a Si atom from the lattice and hence producing a vacancy in the lattice. This vacancy can diffuse through the lattice until it finds a stable state, associating with a dopant atom, impurity or another vacancy. Each trap creates one or more energy levels within the band gap of the silicon. The position of these energy levels within the band gap determines the probability of the capture or release of an electron, subject to Shockley Read Hall theory [38,39]. The emission

time constant of the energy state for the trap in question will vary with temperature and therefore the temperature of operation of the device determines which trap species will have the most impact on the detector operation.

The smearing caused by the traps can, however, be reduced using one or several of the following techniques. The first requires that the device is optimised to reduce the impact of the traps on the signal. This method was recently used on the ESA Gaia mission [40] in which a narrower buried-channel, the Supplementary Buried Channel (SBC), is used for small signals such that the electrons occupy a smaller volume and therefore encounter fewer traps [41]. The second method involves the optimisation of device operation. Through carefully choosing the device temperature or the way in which the device is operating, it has been shown that the effect of the radiation-induced traps can be reduced dramatically [42,43]. The third method involves the correction of smeared images through post-processing [36,44,45], as shown in Figure 1, making use of models of the charge transfer in the CCD in the presence of traps [44-47]. This correction is usually required alongside the optimisation of the device design and device operation to reach the level of correction required.

As the science goals of space missions become ever more demanding on the detectors implemented in the focal plane, more detailed and accurate correction against the disturbance caused by the traps is required. As an example, a 90% correction was achieved for HST in 2006, and more recently increased to 97% through the use of an updated mode [44]. The correction required for the VIS imager on the ESA Euclid mission [48-50] is of the order of 99% [48,50,51]. In order to provide this level of correction, more detailed models of charge transfer through a radiation damaged CCD are required, and in order to do so, one must dramatically

improve the knowledge of, and accuracy of, the understanding of charge storage in the CCD [52,53] and properties of the traps present.

The formation of the A-centre in silicon is of particular importance to the operation of CCDs in many space applications. At an operational temperature around -120 ºC, the A-centre has an emission time similar to the transfer rate in the serial register of the device [42]. The trap therefore interferes with the readout process, transferring signal by one or more pixels against the direction of transfer through the device.

Although there have been many studies of the effects of radiation damage in CCDs [54-58] one must begin to understand traps to a much deeper level, moving towards the characterisation to the individual trap level [59]. Whilst this level of analysis has recently been achieved experimentally [60,61] through the process of "single-trap pumping", as shown in Figure 2, the results produced demonstrate that there is still much that is unknown about the A-centre itself and therefore further research in this area is of high importance.

3. Oxygen-vacancy defects in silicon

A. The A-centre

Upon irradiation of Si, at room temperature vacancies and self-interstitials form. Both are very mobile, although most are destroyed upon annihilation ($V + Si_I \rightarrow 0$). The remaining vacancies either pair together to form divacancies (V_2) or are captured by impurities present in the Si lattice. Oxygen in Si is a very efficient trap for vacancies leading to the formation of the *V*O. The defect is formed when a migrating vacancy approaches an oxygen interstitial atom and a first neighbour Si lattice atom is ejected. The following model for the negative charge state of the defect structure was

suggested by EPR measurements [62] performed ~50 years ago. From the initial four broken bonds around the vacancy (corresponding to the four Si atoms surrounding it) two are bridged by an oxygen atom to form a Si-O-Si molecule. The other two Si atoms form a weak Si-Si molecular bond (Figure 3). In this structure the oxygen atom is attached to the dangling bonds across the silicon vacancy forming the *V*O defect with C_2v symmetry. The latter bond between the two Si atoms has the capacity to trap an electron and is responsible for the electrical activity of the defect. From EPR measurements [62] it was determined that the wavefunction of the unpaired electron is highly localized, being ~70% on the Si-Si bond. This leads to the introduction of an acceptor level reported at E_c – 0.17 eV in the band gap. Uniaxial stress studies have determined that the defect has also a neutral charge state with a similar structure [63]. Recent theoretical investigations based on density functional theory employing hybrid functionals indicate that the defect possesses both a neutral and a double negative charge state [64]. The geometrical configuration of the defect could be considered as a nearly-substitutional oxygen atom. In reality, the oxygen atom is slightly further away from the vacancy site (~0.9 Å) along the <100> direction [65]. The defect is infrared-active with an absorption band at 830 cm^{-1} related to the neutral charge state [66] and an absorption band at 885 cm^{-1} related to the negative charge state [67]. The band originates from the antisymmetric-stretching vibrational B_1 mode of the oxygen atom in the Si_2O molecule of the *V*O structure in the neutral and the negative charge state of the defect respectively. Density functional calculations [68] have concluded that in the negative charge state the oxygen atom is displaced away from the reconstructed bond in agreement with the idea that the additional electron is trapped in this bond and repels the negatively polarized oxygen atom. Due to this movement, the bonds around the oxygen atom are compressed leading to a higher local vibrational mode (LVM)

frequency in comparison to that of the neutral charge state. Additionally, two bands at 1370 and 1430 cm^{-1} have been attributed to a combination of the antisymmetric B_1 stretching mode and the symmetric stretching mode A_1 in the two charge states respectively of the *V*O defect [69].

B. The VO_2 defect

The VO_2 defect is mainly formed in irradiated Si when, at ~300 ^oC, the *V*O centres begin to migrate and are trapped by oxygen atoms ($VO + O_i \rightarrow VO_2$). The VO_2 structure (Figure 4) has D_{2d} symmetry with the two oxygen atoms sharing a vacancy site. Each of the two oxygen atoms is bonded with two silicon atoms of the vacancy. In this arrangement the two oxygen atoms are repulsed from the vacancy. Thus, in comparison with the *V*O defect, the O-*V* distance increases in the VO_2 defect. Since for the same space two oxygen atoms are now accommodated in the vacancy site the lengths of the Si-O bonds become shorter in the VO_2 defect than those in the *V*O defect. This leads to a higher vibrating frequency. Indeed the LVM frequency of the VO_2 structure is found experimentally at ~ 890 cm^{-1} which is larger than that of ~ 830 cm^{-1} of the *V*O defect. On the other hand, the two oxygen atoms in the VO_2 structure bridge all four dangling bonds, namely two bonds for each oxygen atom. Accordingly, all these dangling bonds are passivated, making the defect electrically inactive. The centre has been studied [68,70-73] extensively both experimentally and theoretically, exhibiting a number of important properties including metastability [74,75]. On the other hand, it is also technologically important due to the role it plays in oxygen precipitation processes [76].

C. Insights from density functional theory

As can be deduced from the previous experimental studies, the A-centre can exist at different charge states depending on the position of the Fermi level in the band gap [62,67]. In a recent study, Wang *et al.* [64] employed hybrid density functional theory to gain a fundamental understanding of A-centres in silicon. The calculated formation energy of the defect with respect to the Fermi energy for all possible charge states is given in Figure 5, whereas the transitions levels for the *V*O and *V* defects are summarized in Table 1 [64]. Note that the transition levels of Table 1 were derived from Fig. 5 at the Fermi energy point where the respective formation energies cross [64]. From Fig. 5, it is clear that only two charge states of the A-centre are important. The VO^{0} defect is energetically favourable up to a Fermi energy of 0.54 eV, above which the VO^{-2} defect becomes favourable. At this point we should consider that DFT results apply to a temperature of 0 K, whereas experimental studies are typically performed at higher temperatures. Bean and Newman [67] determined that an increase of the temperature will effectively lower the position of the Fermi level in the band gap and therefore reduce the fraction of the VO^{-1} with respect to the VO^{0} defect. In many previous DFT studies the VO^{0} and VO^{-1} defects were studied, however, the VO^{-2} was not considered (for example [68]). Pesola *et al.* [70], employing DFT within the local density approximation (LDA), considered VO^{-2} and calculated that it is prevalent for Fermi energies above 0.53 eV in agreement with the hybrid DFT study of Wang *et al.* [64] (refer to 0.53 eV for configuration (-,--) in Table 1). Hybrid density functional theory is a more appropriate theoretical technique as compared to the local density approximation [64]. The LDA, or the more evolved generalised gradient approximation (GGA), are far more computationally economical approaches as compared to hybrid DFT, however, they lead to an inappropriate description of group IV elemental semiconductors including a severe underestimation of their band gaps

and other properties (for example, formation and binding energies, especially of charged defects) [77-79].

Wang *et al.* [64] also considered the formation energies of the *V* and O_i defects, which are the constituents of the *V*O defect, with respect to the Fermi energy and a number of charge states. As it can be observed from Figure 6(a) the vacancy formation energy is large (around 4.5 eV) at low Fermi energy [64]. Above a Fermi energy of 0.27 eV the -2 charge state is prevalent and the vacancy formation energy decreases to about 3 eV [64]. The high vacancy formation energy in Si is consistent with experimental results concerning silicon crystal growth, Si self-diffusion, and dopant diffusion studies [77,80]. In a radiation environment it is logical to consider a supersaturation of vacancies, which will effectively enhance the formation of A-centres. In Figure 6(b) it is clear that the neutral charge state is energetically favourable for the O_i defect (formation energy of 1.95 eV) [64], consistent with previous DFT studies [70]. Taking into account the above vacancy and oxygen interstitial formation energies one may consider that the formation of the VO^0 and VO^{-2} pairs can occur via the $V^0 + O_i \rightarrow VO$ and $V^{-2} + O_i \rightarrow VO^{-2}$ reactions, respectively [64].

4. Impact of isovalent doping

A. Background

Various approaches and techniques have been used and suggested over the last fifty years with the aim of improving the Si material and thus enhancing the yield and performance of Si-based devices. Important among them, primarily from the angle of defect engineering, is isovalent doping [81-85]. Carbon (C), germanium (Ge), tin (Sn) and lead (Pb) together with Si form group IV of the periodic system. Since they are

isoelectronic with Si, their introduction into the lattice does not affect the electrical properties. In other words, the above impurities, being isovalent, can be incorporated at substitutional sites replacing Si atoms and are electrically inactive. Carbon is the lightest of the impurities, having a smaller covalent radius r_C = 0.77 Å compared with that of Si r_{Si} = 1.17 Å. On the other hand, Ge is slightly larger than Si, having a covalent radius r_{Ge} = 1.22 Å , although the heavier of them, Sn and Pb, have covalent radii of r_{Sn} = 1.41 Å and r_{Pb} = 1.44 Å, respectively. As a result of their magnitude, when incorporated in the Si lattice they introduce elastic stresses, tensile for the case of the smaller C and compressive for the case of the larger Ge, Sn and Pb. Isovalent doping has been used in a variety of applications in Si-based technology in relation to the production of defects, especially with regards to radiation-induced defects, the reactions they participate in, the diffusion and aggregation processes of impurities (oxygen and carbon mainly) and the gettering of impurities. The aim therefore is to use isovalent doping to optimise electronic systems.

The main properties and impact of isovalent impurities in Si can be summarised as follows:

1) They are neutral impurities and therefore their introduction in the lattice does not affect the carrier concentration in the Si crystal.

2) They affect, due to the induced stress fields, the equilibrium concentration of intrinsic defects [86], that is, vacancies and self-interstitials.

3) Isovalent dopants can interact either with vacancies or with self-interstitials, depending on the magnitude of their covalent radius, namely if it is larger or smaller than that of the host atom. In the former case (Ge, Sn, Pb), the isovalent dopant acts as an effective sink for vacancies although conversely, in the latter case (C) for self-interstitials. As a result of this tendency, the larger-than-Si isovalent atoms capture

vacancies, thus generally inhibiting or suppressing the formation of stable radiation defects such as vacancy-related defects. Important among them in Si is the *V*O centre which, besides the V_2 defects, is a significant recombination centre having detrimental effects on the properties of the material. Besides the production of vacancy-related defects, their thermal stability and reactions with other defects are affected [87-108]. This shows the potential of the latter impurities for altering the radiation hardness of the Si material.

4) They affect the mechanisms of the diffusion and aggregation processes of various impurities such as oxygen. In this sense, the formation of thermal donors, oxygen aggregation and precipitation processes in Si are substantially affected [18,109-114] by the presence of isovalent dopants.

5) They affect the mechanical properties of Si [115,116].

6) Their presence can modify the carrier's mobility [117] and offers possibilities for bandgap engineering [118], a key point in Si-based technology.

7) They can affect the micro-defect population which is related to the reduction of the thermal budget of devices [82,85], something very important for microelectronics, especially in this era of device miniaturisation.

B. Germanium doping

Ge has a slightly (4%) larger covalent radius than that of Si. Ge is an effective trap for vacancies but only below room temperature (RT). Above ~180K, Ge*V* pairs are unstable [87,88] and dissociate, releasing the vacancies. Above RT Ge acts as an effective channel for indirect annihilation of free components of Frenkel pairs [119,120]. In general, Ge affects the introduction rate of *V*O and V_2 defects and their thermal stability [119,121,122]. More specifically, it suppresses the formation of *V*O

and V_2 defects and, whilst reducing the thermal stability of the *V*O defect, will act to enhance that of the V_2 defect. Notably, in Si with high Ge content, Ge acts [99,123] as a self interstitial trapping impurity and in this case could enhance *V*O concentration.

Ge diffusion in Si was studied in [81] detail as a means for indirect investigation of self-diffusion. Ge doping has been found to retard and suppress thermal donor formation [123,124] thus stabilizing the electrical properties of Si wafers. On the other hand, Ge enhances [99,124,125] the generation of oxygen precipitates, thus improving the internal gettering capability of the material for metallic contaminants. The latter property, together with the enhancement of the mechanical strength of the corresponding wafers, largely improves the capability of Si for photovoltaic applications.

Ge codoping with Ga, As, P and B modifies the Si material properties and affects PV characteristics [126-129]. Importantly, it improves the diffusion segregation redistribution of boron and phosphorus during thermal oxidation of Si and also suppresses the formation of boron-oxygen defects [127,130]. The presence of the latter defects in solar cells causes significant degradation of carrier lifetime, leading to a 2-3% loss of the energy conversion efficiency of the cell. Notably, the lifetimes of minority charge carriers [131] in B-doped Cz-Si crystals are increased.

Ge doping improves the mechanical strength of Si wafers by retarding dislocation movement and precipitation in the bulk [82,116]. Interestingly, Ge alone, and/or by codoping with C, causes suppression of large-size voids leading to their elimination [82,109,132,133]. Importantly, voids and oxygen precipitates generate leakage currents in electronic devices [82]. Moreover, oxygen precipitates are strong recombination centres [134], thus deteriorating the efficiency of solar cells. Their control is a crucial issue in Si-based electronic industry.

C. Tin doping

Sn dopants not only trap vacancies and affect vacancy-related defects [88,91,95,135] but also affect the generation rate of interstitial-related defects in Si [136-139]. Indeed, besides Sn*V* pairs, SnC_i pairs also form in irradiated Si. Since carbon and tin preferentially trap self-interstitials and vacancies respectively, material codoping with Sn and carbon has been proposed as a tool to assess the degradation of Si-based devices [88].

Sn suppresses [88,96] the formation of *V*O and V_2 defects in irradiated Si. Both defects introduce electrical levels in the gap which act as recombination centres with deleterious effects on device performance. Thus, Sn appears as a potential candidate to improve radiation hardness of Si material for applications in solar cells and detectors. However, besides the suppression of the *V*O and V_2 defects, the Sn*V* defect formed also introduces [88,110] electrical levels in the gap with the recombination ability of charge carriers. This diminishes the effectiveness of Sn for material hardening [97,140] and one should assess the overall effect of the presence of Sn in the lattice to be able to properly make use of the hardening potential of Sn in Si for certain applications. Furthermore, Sn has been used as a tool to investigate [92,141,142] the production of *V*O, V_2 and carbon related defects in Si, as well as the suggestion of the effect of *V*O in the radiation-enhanced diffusion of oxygen in Si. Reactions between extended defects and impurities in Si containing high oxygen precipitation have been investigated with the help of tin doping [143]. Shallow junction formation by preamorphisation with Sn implantation has also been reported [144]. Comparisons of the different geometry of Sn*V* with Ge*V* and V_2 have also been discussed in the literature [1,140].

Notably, Sn has a strong influence on the generation and annealing of oxygen thermal donors as well as on oxygen aggregation and precipitation processes in Si [19,110,112,145].

D. Lead doping

Pb has shown an ability to capture vacancies and thus affect the production of vacancy-related defects, although the picture is not as complete for this element since a signal from the Pb*V* pair has not yet been detected. In any case, although the effect of lead in radiation induced defects has been studied as systematically as Ge or Sn, it has been found [98,105-107,146,147] that Pb, mostly in codoping with C to relieve the strains in the lattice, suppresses the formation of the *V*O defect, affects its thermal stability and reduces its conversion to the VO_2 defect. Additionally, it has been determined [20,148] that Pb has an influence on the density of growth of microdefects and on the lifetime of non-equilibrium current charge carriers, as well as on the formation of thermal donors and oxygen precipitates.

E. Carbon

Although the ability of carbon to trap vacancies is well-established, its propensity to do so is still an open issue in the literature. The formation of C*V* pairs has been investigated [149-153] both experimentally and theoretically in the literature but there is no definite conclusion about their existence. Carbon also affects the production and evolution of vacancy-oxygen defects in irradiated Si [154-156]. It affects oxygen aggregation processes in Si in general, suppressing the thermal donor formation and enhancing oxygen precipitation, although the overall effect depends on the temperature range of the thermal treatments [157-159].

Carbon codoping with Ge in Si leads [84,161] to void elimination and enhances the internal gettering capability and the potential applications for integrated devices. C codoping with Sn in Si, due to the induced strain compensation, has potential applications in devices with enhanced resistance [88,136] when operating in a high radiation environment. Sn-doped Si containing a high carbon concentration appears [110] very useful for a special kind of light-emitting diode that is valuable for Si-based optical interconnects on-chip. C codoping with Pb in Si has been used [160] to retain the Pb atoms at substitutional sites and suppress any Pb precipitation in the Si lattice [161]. Also, Pb and C codoping suppresses *V*O formation more than with C-doped Cz-Si [105-107,146,147]

F. Insights from density functional theory

DFT studies are a valuable tool in the study of dopant-defect interactions in semiconductors, including the interactions between oversized dopants and defects in group IV semiconductors [162-170]. Recent DFT studies have investigated the impact of isovalent dopants on the stability of vacancy-oxygen defects in Si [171]. Considering first of all O_i, it is evident from previous DFT calculations that these do not bind with isovalent impurities at nearest neighbour sites (refer to [171] and references therein). The introduction of isovalent dopants (C, Ge, Sn) with the A-centres is attractive, leading to the formation of *DV*O defects via the reaction $D + VO \rightarrow DVO$. The stability of these *DV*O defects is higher in comparison to the *V*O defects [171]. Sn*V*O defects are significantly more strongly bound when compared to Ge*V*O and C*V*O defects [171].

G. Trends

Irradiation experiments [88] have provided strong evidence of the tendency of Sn to capture vacancies but not Si_I defects. It has also been determined [142] that Sn does not form bonds with oxygen atoms, at least in nearest-neighbour locations. All of these properties have led [172] to the suggestion of using Sn as a way to tune vacancy and interstitial-related reactions. Thus, Sn has been used to establish whether an unidentified defect is vacancy or interstitial related, as for instance in the case of the V_2 and C_iO_i defects [92,141]. Sn's potential to trap vacancies in Si leads to the suppression of the formation of vacancy-related radiation induced defects and this constitutes Sn as a beneficial dopant for the radiation hardness of Si for several applications such as detectors and solar cells. However, the electrical activity of Sn*V* pairs creates channels for recombination activity, which can be generally harmful for the operation of devices. Remarkably, DLTS and PL measurements have verified [97,173,174] that Sn doping suppresses the formation of *V*O and V_2, as with P*V* pairs (E-centres), in *n*-type doped Si; these are important recombination centres. It has also been shown [97,173,174] that the recombination activity of the Sn-related radiation defects is low. This means that the recombination activity is better controlled when Si is doped with Sn and as a consequence the quality of the material is improved. There is, however, a delicate balance between the suppression of harmful radiation defects and the formation of electrically active Sn-related complexes. Considering for example Si detectors, a detailed understanding of the behavior of Sn is required to assess its utility and optimize the operation of the device. It is also important to take into account the presence of carbon in Si. Co-doping with Sn and C has been suggested [88] as a way to compensate strains induced in the Si lattice due to the larger covalent radius of Sn as compared to Si. Notably, although Sn practically does not interact with self-interstitials, it interacts with interstitial related defects such as C_i

to form C_iSn pairs [136,175] which are electrically active. Fortunately, the C_iSn pairs anneal out at room temperature and therefore essentially do not significantly influence the operation of the relative devices. In a recent study [104], it was determined (refer to Figure 7) that in Sn-rich samples there is a large decrease in the *V*O defect concentration in comparison with that in Sn-poor samples, especially at temperatures below ~170 ^{o}C. However, above this temperature the *V*O concentration increases significantly due to the dissociation of Sn*V* pairs, with the released vacancies pairing with oxygen atoms to form additional *V*O pairs. To unleash the full potential of isovalent doping on defect engineering, and to extend the range where *V*O concentration is low to higher temperatures than 170 ^{o}C, we have studied the relative effect of doping with larger impurities such as Pb, Zr and Hf [104]. Models, in conjunction with DFT theory calculations, led to the suggestion that oversized dopants can extend the temperature range over which the *V*O concentration is low and thus improve the operation of the devices [104].

Further progress on the issue can be achieved by studying the concentration of the A-centre as a function of the covalent radius of the isovalent dopant. Figure 8 [98] represents the evolution with temperature of the *V*O and VO_2 defects for various dopants. In Ge or Pb doped samples the inverse annealing stage of the *V*O defect above the temperature of ~170 ^{o}C does not appear as is in the case of Sn-doped Si. This is due to the fact that, in Ge-doped Si, the Ge*V* pairs [87] are unstable above 200 K (well below room temperature). Notably, the thermal stability of Ge*V* pairs turned out [176] to be dependent on Ge concentration. On the other hand, in Pb-doped Si DFT calculations indicated [104] that the Pb*V* pair has a larger binding energy, and in effect a larger thermal stability, than that of the *V*O defect therefore any additional formation of *V*O pairs up to 350 ^{o}C may not occur as a result of Pb*V* formation.

Interestingly, no LVM band related to the Pb*V* defect has been reported so far [96,105].

The next point to be discussed is the effect of the size of the isovalent dopant on the production of the *V*O defect. Figure 9 presents the concentration of the *V*O defect with respect to the covalent radius of the isovalent dopants (C, Ge, Sn and Pb) [105]. Two samples with low and high carbon concentration are depicted to indicate the effect itself in *V*O production and used as a reference for comparison purposes since carbon is present in all the other Ge, Sn and Pb samples. The impact of carbon is shown in Figure 10 and it will be discussed below. Notably, the two Ge-doped samples with high and low Ge concentration behave differently [99] when at concentrations ~ 10^{20} cm^{-3} as opposed to concentrations below ~5 x 10^{19} cm^{-3}. In other words, the influence of Ge in the availability of vacancies in the course of irradiation is different between the samples with high and low Ge concentration, therefore its effect in the *V*O production is different [99]. In particular in Si with high Ge content, *V*O production is enhanced although in Si with low Ge content the *V*O content is suppressed. An additional Si sample codoped with Sn and Pb is also shown for completeness. As a general trend, it is observed that the production of *V*O defects decreases with the increase of the covalent radius of the dopant impurity. The larger the size of the isovalent dopant (Ge, Sn and Pb), the smaller the concentration of the *V*O defect. The phenomenon is attributed to strains induced in the Si lattice due to the introduction of oversized impurities. These strains tend to relax through the capture of vacancies with the larger dopant atom having a higher propensity to capture vacancies. As a result, the competition with oxygen in trapping vacancies is enhanced, leading to a decrease in the *V*O concentration. In Figure 10, the observed increase in *V*O production with increased carbon concentration is attributed to the greater

efficiency of the latter impurity to trap self-interstitials. This results in an increase of the availability of vacancies during irradiation and therefore an enhanced productivity of *V*O defects. Apparently, the larger the concentration of carbon, the larger the trapping of self-interstitials, hence a larger number of vacancies are available to be captured by oxygen atoms. In Figure 10, for samples with approximately the same carbon concentration (for instance ~ 10^{17} cm^{-3}), the larger the dopant impurity the smaller the *V*O production in agreement with the trend depicted in Figure 9.

At approximately 300 ^{o}C the *V*O defect becomes unstable and converts to the VO_2 defect. The main reactions that govern the above transformation process are: *V*O + $O_i \rightarrow VO_2$ and *V*O + $Si_I \rightarrow O_i$. The first describes the migration of *V*O and its capture by oxygen atoms to form the VO_2 defect, although in a parallel second reaction running simultaneously with the first, a percentage of *V*O pairs are destroyed by self-interstitials to produce oxygen interstitials. The percentage of *V*O pairs converted to VO_2 defects is presented by the conversion ratio [VO_2] / [*V*O] and Figure 11 shows this ratio as a function of the covalent ratio of the isovalent dopants. It is immediately seen that the conversion ratio decreases with the increase of the covalent radius or in other words the larger the size of the isovalent dopant the fewer *V*O defects that convert to VO_2 defects. The phenomenon was attributed [98,106] to the effect of strains induced by oversized dopants on the availability of self-interstitials which affects the second reaction above and therefore the balance between the two reactions, leading finally to a reduction of VO_2 formation with the increase of the covalent radius of the isovalent dopant. In particular, we have suggested [101] that due to the introduction of large substitutional isovalent dopants the induced strains cause an enhanced release of self-interstitials. Sources of these self-interstitials are small defect clusters of interstitial-type formed in Cz-Si in the course of irradiations

[177]. We argue that the strains affect the binding of these self-interstitials in the clusters. More specifically, it is their binding energy that is affected and most possibly reduced due to the strains [178]. As a result, the liberation of these self-interstitials is facilitated to occur at a lower temperature and more intensively leading to an enhancement of the reaction $VO + Si_I \rightarrow O_i$ over the reaction $VO + O_i \rightarrow VO_2$. Of course carbon, being present in Cz-Si, is a strong trap of self-interstitials, affecting also the above process and this is depicted in Figure 12 which shows that the conversion ratio $[VO_2]/[VO]$ decreases with an increase in the carbon concentration. However, for samples with approximately the same carbon concentration (for instance ~ 10^{17} cm^{-3}), the larger the dopant impurity the smaller the percentage of *V*O pairs converted to VO_2 defects, consistent with the trend depicted in Figure 11.

Remarkably, the thermal stability of A-centres is also affected by the introduction of isovalent dopants in the Si lattice. This is observed in Figure 8, where *V*O anneals out at a lower temperature in Pb-doped Si than that for Sn-doped Si. In previous studies [98,105-108] there were not enough samples with an adequate number of various Sn and Pb concentrations to deconvolve the exact effect of Sn and Pb and therefore make appropriate comparisons. Conversely, there were studies with numerous Ge-doped samples with concentrations spanning three orders of magnitudes ($1x10^{17}$ cm^{-3}-$2x10^{20}$ cm^{-3}) [101]. In these studies it is interesting to consider the impact of Ge dopant concentration on the stability of the *V*O, and the emergence of the VO_2, defect. Figure 13 shows the annealing temperature of the *V*O defect (a) and the formation temperature of the VO_2 defect (b) respectively in relation to the Ge concentration [101]. It is observed that both the temperatures characterizing the onset of the annealing of the *V*O defect and the onset of the growth of the VO_2 defect decrease with the increase of the Ge concentration. Both observations can be

considered as being due to the strains induced in the Si lattice by the presence of Ge, in particular among the two main reactions that participate in *V*O annealing and VO_2 formation, namely: $VO + O_i \rightarrow VO_2$ and $VO + Si_I \rightarrow O_i$. The induced strains affect the binding of self-interstitials in the larger self-interstitial clusters that provide them [177,179], somehow controlling their liberation. It is envisaged that the larger the Ge concentration, and therefore the larger the induced strains, the easier the liberation of the self-interstitials. This makes the onset of the second reaction occur at a lower temperature which is manifested by the onset of the annealing of the *V*O defect at a lower temperature. This is also in agreement with the observed emergence of the VO_2 defect at a higher temperature than that of the corresponding onset of the annealing of the *V*O defect. In fact the second reaction is related with the destruction of the *V*O defect occurring in the first stage of its annealing, although the formation of the VO_2 defect is related with the first reaction taking place [177,180] at a later stage.

H. Perspectives and defect engineering strategies

From a practical point of view, for the case of vacancy-oxygen defects it is much easier, instead of trying to completely eliminate them, to live with them and find ways to control their electrical properties. In this respect DFT calculations can provide insights that can support and complement experimental methods. Importantly, experimental and DFT studies are consistent in that large isovalent atoms can impact the formation of A-centres in Si. The key to this is that A-centres, and in particular the *V*, relieve the strain introduced in the lattice by the large isovalent substitutional atoms. The introduction of these oversized atoms is an effective defect engineering strategy to suppress the formation of *V*O defects. A key element of defect engineering strategies requires controlling the formation of both vacancies and self-interstitials.

Their balance was demonstrated in recent studies (refer to [181] and references therein). Initial DFT work [104] suggests that large isovalent impurities such as hafnium and zirconium can be very effective in constraining A-centres, although these results need to be validated experimentally. An important factor to consider is the concentration of the dopant atoms. To be effective, the proposed defect engineering strategies require that isovalent atoms have a concentration comparable to that of A-centres in undoped Si. Finally, it should be noted that when considering the formation of devices, the impact of non-equilibrium conditions during manufacturing can impact the results. For example, free surfaces can lead to a *V*-Si_I imbalance and this must be understood in detail as the Si surface properties can strongly affect defect reactions.

Isovalent dopants can affect oxygen aggregation processes in Si, more specifically suppressing thermal donor formation and enhancing oxygen precipitation. Carbon aggregation is also affected. To this end, it is highly important to understand the effect of isovalent doping on the production of oxygen-related defects, the reactions in which they participate upon annealing, and their conversion to other complexes at higher temperatures. This is highly desirable in order to enhance the capability of various Si-based devices.

The present review highlights strategies that may inspire experiments. For example, the impact of isovalent dopants such as Sn and Pb on the A-centre can inspire the study of Hf and Zr that were identified by DFT as potentially important isovalent dopants. Future work should also study the conditions under which these isovalent dopants are soluble and whether they form clusters, precipitates or other defects that can degrade the performance of the devices.

Finally, it is of interest to consider related defects and strategies in other semiconductor materials such as Ge and group IV binary (for example $Si_{1-x}Ge_x$, Sn_{1-}

$_xGe_x$ or $Si_{1-x}Sn_x$) and ternary (for example $Si_{1-x-y}Ge_xSn_y$) alloys [182-204]. In the past few years these materials are becoming increasingly important given their advantageous materials properties (increased charge carrier mobilities, lattice matching to other substrates, band gap engineering etc) and are applicable in nanoelectronic devices [189]. At any rate dopant-defect interactions in binary and ternary alloys are a relatively unchartered area of research and as such the present review can inspire further experiments to confine the deleterious defects [193,196-199].

5. Summary

Isovalent dopants such as Ge, Sn and Pb affect reactions between oxygen and vacancies and consequently affect the production of oxygen-vacancy related defects. These dopants also impact the thermal stability of defects and the conversion to next generation defects upon thermal annealing. More specifically, all three isovalent dopants Ge, Sn and Pb, either alone or in codoping with C, are very promising for material hardening relating to radiation as well as for increasing the thermal resistance in relation to the stability of the formed defects. In the present review we have discussed results mainly from IR spectroscopy measurements and density functional calculations in a twofold attempt: firstly, to introduce models to explain the overall effect of the presence of isovalent dopants in the Si matrix on the behaviour of radiation and thermal defects related mainly to O, and secondly, to suggest defect engineering strategies on the purpose of preparing Cz-Si material with enhanced radiation hardness and to improve thermal resistance.

Overall, the presence of isovalent dopants has a significant impact on the mechanisms and the processes that lead to the formation of the vacancy-oxygen

defects. The mechanisms that affect the production, thermal stability and annealing of these defects are subject to the influence of the size of the isovalent dopant due to the induced strain fields. In general, the larger the covalent radius of the dopant the smaller the rate of production of the *V*O defect and also the lower the percentage of *V*O defects that are transformed to VO_2 defects. The thermal stability of *V*O defects is also reduced due to the presence of the dopants. For Ge-doped Si in particular, it was found that the larger the concentration of Ge the lower the thermal stability of the *V*O defect. Also, it was found that for large Ge content (above 10^{20} cm^{-3}) the induced strain fields in the lattice tend to enhance the production of *V*O defects, although for Ge content smaller than $5x10^{19}$ cm^{-3} *V*O production is reduced. Finally, our results indicate that isovalent doping could be beneficially used for applications requiring radiation tolerant Si material, in cases for instance of radiation detectors, solar cells and generally when the relating devices operate in high level radiation environments.

References

1. G. D. Watkins, Mater. Sci. Semicond. Process. **3**, 227 (2000).

2. L. C. Kimerling, Radiation Effects in Semiconductors,1976, 10P Conf. Ser. No 31, eds. N. B. Urli and J. W. Corbett (Institute of Physics, Bristol 1977) p. 221.

3. S. D. Brotherton and P. Bradley, J. Appl. Phys. **53**, 5720 (1982).

4. W. M. Chen B. Monemar, and E. Janzen, J. L. Lindstrom, Phys. Rev. Lett. **67**, 1914 (1991).

5. A. M. Frens, M. T. Bennebrock, A. Zakrzewski, and J. Schmidt, W. M. Chen, E. Janzen, J. L. Lindstrom and B. Monemar Phys. Rev. Lett. **72**, 2939 (1994).

6. A. Khan, M. Yamaguchi, Y. Ohshita, N. Gharmarasu, K. Araki, T. Abe, H. Ohshima, M. Imaizumi and S. matsuda J. Appl. Phys. **90**, 1170 (2001).

7. L. F. Makarenko, Semiconductors **34**, 1112 (2000).

8. L. F. Makarenko, Semicond. Sci. Technol. **16**, 619 (2001).

9. G. D. Watkins, Semicond. Sci. Technol. **6**, B111 (1991).

10. F. Shimura (Ed.) Oxygen in Silicon, Semiconductors and semimetals, edited by (Academic, San Diego, 1994), Vol. **42** (and references therein).

11. A. S. Oates and R. C. Newman Appl. Phys. Lett. **49**, 262 (1986).

12. R. C. Newman, J. Phys.: Condens. Matter **12**, R335 (2000).

13. A. Ourmazd, W. Schoter, and A. Bourret, J. Appl. Phys. **56** ,1670 (1984).

14. R. C. Newman, A. K. Tipping and J. H. Tucker, J. Phys. C: Solid State Phys. **18**, L861 (1985).

15. F. Shimura, T. Highuchi, and R. S. Hockett, Appl. Phys. Lett. **53**, 69 (1988).

16. R. C. Newman, J. H. Tucker, A. R. Brown and S. A. McQuaid , J. Appl. Phys. **70**, 3061 (1991).

17. D. Yang, J. Chu, J. Xu and D. Que , J. Appl. Phys. **93**, 8926 (2003).

18. J. Chen, D. Yang, X. Ma, R. Fan, and D. Que, J. Appl. Phys. **102**, 066102 (2007).

19. C. Ghao, X. Ma, J. Zhao, and D. Yang J. Appl. Phys. **113**, 093511 (2013).

20. M. M. Krasko, V. V. Voitovych, M. V. Neimash, A. M. Kraitchinskii, Ukr. J. Phys. **49**, 691 (2004).

21. U. Gösele, T. Y. Tan, Appl. Phys. A **28**, 79 (1992).

22. T. Sinno, J. Dai and S. S. Kapur, Mater. Sci. Eng. B **159-160**, 128 (2009).

23.R. Falster and V. V. Voronkov, Mater. Sci. Eng. B **73**, 87 (2009).

24**.** T. Umeda, Y. Mochizuchi, K.Okonogi and K. Hamada, Physica B **308-310,** 1169 (2001).

25**.** T. Umeda, K. Ohyu,S. Tsukada, and K. Hamada ,S. Fujieda, and Y. Mochizuchi, Appl. Phys. Lett. **88**, 253504 (2006).

26. K. Gill, G. Hall, and B. MacEvoy, J. Appl. Phys**. 82**, 126 (1997).

27. A. Hallen, N. Keskitalo, F. Masszi and V. Nagl, J. Appl. Phys.**79**, 3906 (1996).

28. I. Murin, J. L. Lindstrom, V. P. Markevich, A. Misiuk and C. A. Londos, J. Phys.: Condens. Matter **17**, S2237 (2005).

29. T. Hallberg and J. L. Lindstrom, J. Appl. Phys. **72**, 5130 (1992).

30.V. Akhmetov, G. Kissinger, and W.von Ammon, Physica B **404**, 4572 (2009).

31. B. Surma, C. A. Londos, V. V. Emtsev, A. Misiuk, A. Bukowski, and M. S. Potsidi, Mater. Eng. B **102**, 339 (2003).

32. V. V. Voronkov and R. Falster, J. Electrochem. Soc. **149**, G167 (2002).

33. P. Wagner and J. Hage, Appl. Phys. A **49**, 123 (1989).

34. R. A. Casali, H. Rucker, and M. Methfessel, Appl. Phys. Lett. **78**, 913 (2001).

35. G. R. Hopkinson, "Radiation effects on CCDs for spaceborne acquisition and tracking applications," Radiation and its Effects on Devices and Systems, 1991. RADECS 91, First European Conference pp.368, 372, 9-12 Sep 1991, doi: 10.1109/RADECS.1991.213573

36. D. Burt, J. Endicott, P. Jerra, P. Pool, D. Morris, A. Hussain, P. Ezra, Proc. SPIE 7439, Astronomical and Space Optical Systems, 743902 (August 26, 2009); doi:10.1117/12.825273.

37. R. Massey, Mon. Not. R. Astron Soc. **409**, L109 (2010).

38. W. Shockley and W. T. Jr. Read, Phys. Rev. **87**, 835 (1952).

39. R. N. Hall, Phys. Rev. **87**, 387 (1952).

40. L. Lindegren, C. Babusiaux, C. Bailer-Jones, U. Bastian, A. G. A. Brown, M. Cropper, E. Hg, C. Jordi, D. Katz, F. van Leeuwen, X. Luri, F. Mignard, J. H. J. de Bruijne and T. Prusti, "The Gaia mission: science, organization and present status", IAU Colloq., vol. 248, pp. 217-223, Jul. 2008.

41. G. M. Seabroke, T. Prod'homme, N. J. Murray, C. Crowley, G. Hopkinson, A. G. A. Brown, R. Kohley and A. Holland, Mon. Not. R. Astron Soc. **430**, 3155 (2013).

42. D. Hall, J. Gow, N. Murray and A. Holland, IEEE Trans. Electron. Dev. **59**, 1099 (2012).

43. N. J. Murray, A. D. Holland, J. P. D. Gow, D. J. Hall, J. H. Tutt, D. Burt and J. Endicott, Proc. SPIE **8453**, 845317 (2012).

44. R. Massey, C. Stoughton, A. Leauthaud, J. Rhodes, A. Koekemoer, R. Ellis and E. Shaghoulian, Mon. Not. R. Astron Soc. **401**, 371 (2010).

45. A. Short, C. Crowley, J. H. J. de Bruijne and T. Prod'homme, Mon. Not. R. Astron Soc. **430**, 3078 (2013).

46. R. Massey, T. Schrabback, O. Cordes, O. Marggraf, H. Israel, L. Miller, D. Hall, M. Cooper, T. Prod'homme, and S. M. Niemi, Mon. Not. R. Astron Soc. (submitted).

47. D. Hall, A. Holland, N. Murray, J. Gow, and A. Clarke, Proc. SPIE, **8453**, 845315, (2012).

48. R. Laureijs, J. Amiaux, S. Arduini, J. Auguéres, J. Brinchmann, R. Colem
M. Cropper, C. Dabin, L. Duvet, A. Ealet, et al. (2011, Oct). Euclid Definition Study Report, ArXiv e-prints 1110.3193 [Online]. Available: http://arxiv.org/abs/1110.3193.

49. M. Cropper, A. Refregier, P. Guttridge, M. Cropper, A. Refregier, P. Guttridge, O. Boulade, J. Amiaux, D. Walton, P. Thomas, K. Rees, P. Pool, J. Endicott, A. Holland, J. Gow, N. Murray, A. Amara, D. Lumb, L. Duvet, R. Cole, J.-L. Augueres and G. Hopkinson, Proc. SPIE, vol. 7731, Paper 77311J, Jul. 2010.

50. M. Cropper, H. Hoekstra, T. Kitching, R. Massey, J. Amiaux, L. Miller, Y. Mellier, J. Rhodes, B. Rowe, S. Pires, C. Saxton and R. Scaramella, Mon. Not. R. Astron Soc. **431**, 3103 (2013).

51. R. Massey, H. Hoekstra, T. Kitching, J. Rhodes, M. Cropper, J. Amiaux, D. Harvey, Y. Mellier, M. Meneghetti, L. Miller, S. Paulin-Henriksson, S. Pires, R. Scaramella and T. Schrabback, Mon. Not. R. Astron Soc. **429**, 661 (2013).

52. A. Clarke, D. Hall, N. Murray, J. Gow, A. Holland, and D. Burt Proc. SPIE 8860, UV/Optical/IR Space Telescopes and Instruments: Innovative Technologies and Concepts VI, 88600V (September 26, 2013)

53. A. S. Clarke, D. J. Hall, A. Holland, and D. Burt, J. Instrum. **7**, C01058 (2012).

54. J. P. D. Gow, N. Murray, A. Holland, D. Hall, M. Cropper, G. Hopkinson and L. Duvet, J. Instrum. **7**, C01030, (2012).

55. G. R. Hopkinson and A. Mohammadzadeh, Int. J. Hi. Spe. Ele. Syst. **14**, 419 (2004).

56. J. R. Srour, C. J. Marshall and P. W. Marshall, IEEE Trans. Nucl. Sci. **50**, 653 (2003).

57. A. Holland, Nucl. Instrum. Meth. A, **326**, 335 (1993).

58. J. P. D. Gow, N. Murray, A. Holland, D. J. Hall, M. Cropper, G. Hopkinson, and L. Duvet, J. Instrum. **7**, C01030 (2012).

59. J. Rhodes, A. Leauthaud, C. Stoughton, R. Massey, K. Dawson, W. Kolbe and N. Roe, Publ. Astron. Soc. Pac., **122**, 439 (2010).

60. D. J. Hall, N. J. Murray, A. D. Holland, J. Gow, A. Clarke and D. Burt, accepted for publication in IEEE Transactions on Nuclear Science

61. N. J. Murray, D. J. Burt, D. Hall, and A. D. Holland, Proc. SPIE 8860, UV/Optical/IR Space Telescopes and Instruments: Innovative Technologies and Concepts VI, 88600H (September 26, 2013) doi:10.1117/12.2024826

62. G. D. Watkins and J. W. Corbett, Phys. Rev. **121**, 1001 (1961).

63. D. R. Bosomworth, W. Hayes, A. R. L. Spray and G. D. Watkins, Proc. Roy. Soc. A **317**, 133 (1970).

64. H. Wang, A. Chroneos, C. A. Londos, E. N. Sgourou, and U. Schwingenschlögl, Appl. Phys. Lett. **103**, 052101 (2013).

65. B. Pajot, ,Semiconductors an Semimetals, Vol. 42, Oxygen in Silicon, edited by F. Shimura (Academic, London, 1994) p. 191.

66. J. W. Corbett ,G. D. Watkins, R. M. Chrenko, and R. S. McDonald, Phys. Rev. **121**, 1015 (1961).

67. A. R. Bean and R. C. Newman, Solid State Commun. **9**, 271 (1971).

68. J. Coutinho, R. Jones, P. R. Briddon, and S. Öberg, Phys. Rev. B **62**, 10824 (2000).

69. J. L. Lindstrom, L. I. Murin, V. P. Markevich, T. Halberg, B. G. Svensson, Physica B **273-274**, 291 (1999).

70. M. Pesola, J. Von Boehm, T. Mattila, and R. M. Nieminen, Phys. Rev. B **60**, 11449 (1999).

71. J. W. Corbett, G. D. Watkins, and R. S. McDonald, Phys. Rev. **135**, A1381 (1964).

72. B. J. Svensson and J. L. Lindström, Phys. Rev. B **34**, 8709 (1986).

73. G. G. Deleo, C. S. Milsted and J. C. Kralik, Phys. Rev. B. **31**, 3588 (1985).

74. J. L. Lindström, L. I. Murin, B. G. Svensson, V. P. Markevich, and T. Hallberg, Physica B **340-342**, 509 (2003).

75. C. A. Londos, N. Sarlis, L. Fytros, and K. Papastergiou, Phys. Rev. B **53**, 6900 (1996).

76. V. V. Voronkov and R. Falster, J. Appl. Phys. **91**, 5802 (2001).

77. H. Bracht and A. Chroneos, J. Appl. Phys. **104**, 076108 (2008).

78. R. M. Nieminen, Modell. Simul. Mater. Sci. Eng. **17**, 084001 (2009).

79. A. Chroneos, J. Appl. Phys. **105**, 056101 (2009).

80. V. V. Voronkov and R. Falster, Mater. Sci. Eng. B **134**, 227 (2006).

81. P. Pichler, Intrinsic Point Defects, Impurities, and Their Diffusion in Silicon, Computational Microelectronics, Edited by S. Selberherr, Spinger-Verlag Wien 2004

82. X. Yu, J. Chen, X. Ma, D. Yang, Mater. Sci. Eng. R **74**, 1 (2013)

83. T. Sinno, E. Dornberger, W. von Ammon, R. A. Brown, F. Dupret, Mater. Sci. Eng. R **28**, 1491 (2000)

84. D. Yang, J. Chen, X. Ma, D. Que, J. Cryst. Growth **311**, 837 (2009)

85. J. Chen and D. Yang, Phys. Stat. Sol. C **6**, 625 (2009)

86. J. Vanhellemont, M. Suezawa, and I. Yonenaga, J. Appl. Phys. **108**, 016105 (2010)

87. A. Brelot, J. Charlemagne, Radiat. Eff. **9**, 65 (1971)

88. A. Brelot, IEEE Trans. Nucl. Sci. **19**, 220 (1972)

89. J. Chen, J. Vanhellemont, E. Simoen, J. Lauwaert, H. Vrielink, J. M. Rafi, H. Ohyama, J. Weber and D. Yang, Phys. Stat. Sol. C **8**, 674 (2011)

90. C. V. Budtz-Jorgensen, P. Kringhoj, and A. N. Larsen, N. V. Abrosimov, Phys. Rev. B **58**, 1110 (1998)

91.G. D. Watkins, Phys. Rev. B **12**, 4383 (1975)

92. B. G. Svensson, J. Svensson, J. L. Lindström, G. Davies and J. W. Corbett, Appl. Phys. Lett. **51**, 2257 (1987)

93. K. Schmalz, V.V. Emtsev, Appl. Phys. Lett. **65**, 1575 (1994).

94. L. I. Khirunenko, V. I. Shakhovstov, V. K. Shikarenko, L. I. Shpinar, and I. I. Yaskovets, Sov. Phys. Semicond. **21**, 345 (1987)

95. L. I. Khirunenko, O. A. Kobzar, Yu. V. Pomozov, V. I. Shakhovstov, M. G. Sosnin, N. A. Tripachko, V. P. Markevich, L. I. Murin, and A. R. Peaker, Phys. Stat. Sol. (c) **0**, 694 (2003)

96. M. L. David, E. Simoen, C. Clays, V. Neimash, N. Kras'ko, A. Kraitchinskii, V. Voytovych, A. Kabaldin and J. F. Barbot, J. Phys.: Condens. Matter **17**, S2255 (2005)

97. E. Simoen, C. Clays, V. Privitera, S. Coffa, A. N. Larsen, P. Clauws, Physica B, **308-310**, 477 (2001)

98. C. A. Londos, E. N. Sgourou, D. Timerkaeva, A. Chroneos, P. Pochet and V. V. Emtsev, J. Appl. Phys. **114**, 113504 (2013)

99. C.A. Londos, A. Andrianakis, V. Emtsev, H. Ohyama, Semicond. Sci. Technol. **24**, 075002 (2009)

100. C.A. Londos, A. Andrianakis, E.N. Sgourou, V. Emtsev, H. Ohyama, J. Appl. Phys. **107**, 093520 (2010)

101. C.A. Londos, A. Andrianakis, E.N. Sgourou, V. Emtsev, H. Ohyama, J. Appl. Phys. **109**, 033508 (2010)

102. A. Chroneos, C. A. Londos, E.N. Sgourou, J. Appl. Phys. **110**, 093507 (2011)

103. C.A. Londos, E. N. Sgourou, A. Chroneos and V. Emtsev, Semicond. Sci. Technol. **26**, 105024 (2011)

104. A. Chroneos, C. A. Londos, E.N. Sgourou, and P. Pochet, Appl. Phys. Lett. **99**, 241901 (2011)

105. C. A. Londos, D. Aliprantis, E. N. Sgourou, A. Chroneos, and P. Pochet , J. Appl. Phys. **111**, 123508 (2012)

106. C. A. Londos, E. N. Sgourou, and A. Chroneos, J. Appl. Phys. **112**, 123517 (2012)

107. E. N. Sgourou, D. Timerkaeva, C. A. Londos, D. Aliprantis, A. Chroneos, D. Caliste, and P. Pochet , J. Appl. Phys. **113**, 113506 (2013)

108. C. A. Londos, E. N. Sgourou, and A. Chroneos, J. Mater. Sci.: Mater. Electron. **24**, 1696 (2013)

109. J. Chen, D. Yang, H. Li, X. Ma, and D. Que, J. Appl. Phys. **99**, 073509 (2006)

110. C. Claeys, E. Simoen, V.B. Neimash, A. Kraitchinskii, M. Kras'ko, O. Puzenko, A. Blondeel, P. Clauws, J. Electrochem. Soc. **148**, G738 (2001)

111. M. V. Neimash, M. Kras'ko, A. Kraitchinskii, V. Voytovych, O. Kabaldin, V. Tsmots, E. Simoen, C. Claeys, Electrochem. Soc. Proceedings, 2004-05, p. 286.

112. W. Wijaranakula, J. Appl. Phys. **72**, 2713 (1992)

113. C.A. Londos, A. Andrianakis, V. Emtsev, H. Ohyama, J. Appl. Phys. **105**, 123508 (2009)

114. V. V. Emtsev, G. A. Oganesyan, and Y. V. Schmalz, Semiconductors **27**, 1111 (1993)

115. T. Taishi, X. Xuang, I. Yonenaga,, and K. Hoshikawa, Mater. Sci. Semicond. Process. **5**, 409 (2002)

116. J. Chen and D. Yang, X. Ma, Z. Zeng, D. Tian, L. Li, D. Que, and L. Gong, J. Appl. Phys. **103**, 123521 (2008)

117. B. Pejcinovic, L. E. Kay, T. W. Tang, and D. H. Navon, IEEE Trans. Electron. Devices **36**, 2129 (1989)

118. M. Yoshimi, M. Terauchi, A. Nishiyama, O. Arisumi, A. Murakoshi, K. Matsuzawa, N. Shigyo, S. Tomita, and K. Suzuki, IEEE Trans. Electron. Devices **44**, 423 (1997)

119. V. G. Golubev, V. V. Emtsev, P. M. Klinger, G. I. Kropotov, and Yu. V. Shmartsev, Sov. Phys. Semicond. **26**, 328 (1992)

120. A. L. I. Khirunenko, V. I. Shakhovtsov, and V. V. Shumov, Semiconductors **32**, 120 (1998)

121. N. A. Sobolev, M. H. Nazarre, Physica B **273-274**, 271 (1999)

122. Yu. V. Pomozov, L. I. Khirunenko, V. I. Shakhovtsov, and V. I. Yashnik, Sov. Phys. Semicond. **24**, 624 (1990)

123. V.V. Voronkov, R. Falster, C. A. Londos, E. N. Sgourou, A. Andrianakis, and H. Ohyama, J. Appl. Phys. **110**, 09350 (2011)

124. C. Cui, D. Yang, X. Ma, M. Li, D. Que, Mater. Sci. Semicond. Process. **9**, 110 (2006)

125. D. Yang, Phys. Stat. Sol. (a) **202**, 931 (2005)

126. M. Arivanandhan, R. Gotoh, K. Fujiwara, and S. Uda, Appl. Phys. Lett. **94**, 072102 (2009)

127. L. Wang, P. Clancy, C. S. Murthy, Phys. Rev. B **70**, 165206 (2004)

128. O. V. Aleksandrov and N. N. Afonin, Semicond. Sci. Technol. **18**, 139 (2003)

129. Z. Zeng, J. D. Murphy, R. J. Falster, X. Ma, D. Yang, and D. Wilshaw, J. Appl. Phys. **109**, 063532 (2011)

130. X. Yu, P. Wang, P. Chen, X. Li and D. Yang Appl. Phys. Lett. **97**, 051903 (2010)

131. M. Arivanandhan, R. Gotoh, T. Watahiki, K. Fujiwara, Y. Hayakawa, S. Uda, and M. Konagai, J. Appl. Phys. **111**, 043707 (2012)

132. D. Yang, X. Yu, X. Ma, J. Xu, L. Li D. Que, J. Crystal Growth **243**, 371 (2002)

133. D. Yang, M. Kleverman, L. I. Murin, Physica B **302-303**, 193 (2001)

134. J. M. Hwang and D. K. Schroder, J. Appl. Phys. **59**, 2476 (1986)

135. V. B. Neimash, M. G. Sosnin, B. M. Turovskii, V. P. Markevich, V. I. Shakhovtsov, and V. L. Shindich, Sov. Phys. Semicond. **16**, 577 (1982)

136. E. V. Lavrov, M. Fancialli, M. Kaukonen, R. Jones, P. R. Briddon, Phys. Rev. B **64**, 125212 (2001)

137. L. I. Khirunenko, O. A. Kobzar, Yu. V. Pomozov, M. G. Sosnin, N. A. Tripachko, N. V. Abrosimov and H. Riemann, Solid State Phenomena **95-96**, 393 (2004)

138. E. Simoen, C. Clays, V. Neimash, , A. Kraitchinskii, N. Kras'ko, O. Puzenko, A. Blondeel and P. Clauws, Appl. Phys. Lett. **76**, 2838 (2000)

139. A. N. Larsen, J. J. Goubet, P. Mejlholm, J. S. Christensen, M. Fanciulli, H. P. Gunnlaugsson, P. Weyer, J. W. Petersen, A. Resende, M. Kaukonen, R. Jones, S. Oberg, P. R. Briddon, B. G. Svensson, S. Dannefaer, Phys. Rev. B **62**, 4535 (2000)

140. M. Fanciulli and J. R. Byberg, Physica B **273-274**, 524 (1999)

141.G. Davies, A. S. Oates, R. C. Newman, R. Woolley, E. C. Lightowlers, M. J. Binns and J. G. Wilkes, J. Phys. C: Solid State Phys. **19**, 841 (1986)

142. A. S. Oates, M. J. Binns, R. C. Newman, H. H. Tucker, J. G. Wilkes, and A. Wilkinson, J. Phys. C: Solid State Phys. **17**, 5695 (1984)

143. W. Wijaranakula, J. Appl. Phys. **70**, 3018 (1991)

144. M. Delfino, D. K. Sadana, and A. E. Morgan, Appl. Phys. Lett. **49**, 575 (1986)

145. V.B. Neimash, A. Kraitchinskii, M. Kras'ko, O. Puzenko, C. Claeys, E. Simoen, B. Svensson, and A. Kuznetsov, J. Electrochem. Soc. **147**, 2727 (2000)

146. M. L. David, E. Simoen, C. Clays, V. Neimash, N. Kras'ko, A. Kraitchinskii, V. Voytovych, A. Kabaldin and J. F. Barbot, Solid State phenomena, **108-109**, 373 (2005)

147. M. L. David, E. Simoen, C. Clays, V. B. Neimash, N. Kras'ko, A. Kraitchinskii, V. Voytovych, B. Tishchenko and J. F. Barbot, in High Purity Si VIII, Electrochemical Society Proceedings 2004-2005, 395 (2005)

148. V. B. Neimash, V. Voytovych, A. Kraitchinskii, L. I. Shpinar, N. Kras'ko, V. M. Popov, A. P. Pokanevych, M. I. Gorodys'kyi, Yu. V. Panlovs'sky, V. M. Tsmots, O. M. Kabaldin, Ukr. J. Phys. **50**, 492 (2005)

149. G. D. Watkins and J. W. Corbett in Radiation Effects in Inorganic Solids, Discussions of the Faraday Society, no 31, 86 (1961)

150. K. A. Abdullin and B. N. Mukashev, Semiconductors **29**, 169 (1995)

151. C. A. Londos, M. S. Potsidi, E. Stakakis, Physica B **340-342**, 551 (2003)

152. D. Tersoff, Phys. Rev. Lett. **64**, 1757 (1990)

153. A. DalPino Jn, A. M. Rappe, J. D. Joannopoulos, Phys. Rev. B **47**, 12554 (1993)

154. V. V. Achmetov, V. V. Bolotov, Radiat. Eff. **52**, 149 (1980)

155. G. Davies, E. C. Lightowlers, R. C. Newman, and A. S. oates, Semicond. Sci. Technol. **2**, 524 (1987)

156. C. A. Londos, E. N. Sgourou, and A. Chroneos, J. Mater. Sci.: Mater. Electron., **25**, 914 (2014)

157. H. Bender and J. Vanhellemont, in Handbook of Semiconductors, edited by S. Mahajan (North Holland, Amsterdam, 1994) Vol. 3b, p. 1637

158. A. Borgesi, B. Pivac, A. Sassela and A. Stella, J. Appl. Phys. **77**, 4169 (1995)

159. C. A. Londos, M. S. Potsidi, V. V. Emtsev, Phys. Stat. Sol (c), **2**, 1963 (2005)

160. J. Chen, X. Ma, and D. Yang, Solid State Phenomena, **156-158**, 261 (2010)

161. K. Milands, J. Verheyden, T. Banancira, W. Deweerd, H. Pattyn, S. Buckhpan, D. L. Williamson, F. Varmeiren, G. Van Tendeleo, C. Vlekken, S. Libbrechtand C. Van Haesendonck, J. Appl. Phys. **81**, 2148 (1997)

162. M. Diebel and S. T. Dunham, Phys. Rev. Lett. **93**, 245901 (2004).

163. A. Chroneos, H. Bracht, R. W. Grimes, and B. P. Uberuaga, Appl. Phys. Lett. **92**, 172103 (2008).

164. A. Chroneos, R. W. Grimes, and H. Bracht, J. Appl. Phys. **106**, 063707 (2009).

165. H. Tahini, A. Chroneos, R. W. Grimes, U. Schwingenschlögl, and H. Bracht, Appl. Phys. Lett. **99**, 072112 (2011).

166. N. E. B. Cowern, S. Simdyankin, C. Ahn, N. S. Bennett, J. P. Goss, J.-M. Hartmann, A. Pakfar, S. Hamm, J. Valentin, E. Napolitani, D. De Salvador, E. Bruno, and S. Mirabella, Phys. Rev. Lett. **110**, 155501 (2013).

167. H. Höhler, N. Atodiresei, K. Schroeder, R. Zeller, and P. Dederichs, Phys. Rev. B **71**, 35212 (2005).

168. H. A. Tahini, A. Chroneos, R. W. Grimes, U. Schwingenschlögl, and H. Bracht, Phys. Chem. Chem. Phys. **15**, 367 (2013).

169. H. A. Tahini, A. Chroneos, R. W. Grimes, and U. Schwingenschlögl, J. Appl. Phys. **113**, 073704 (2013).

170. A. Chroneos, J. Mater. Sci. Mater. Electron. **24**, 1741 (2013)

171. A. Chroneos and C. A. Londos, J. Appl. Phys. **107**, 093518 (2010).

172. A. Brelot, Radiation Damage and Defects in Semiconductors ed. J. E. Whitehouse (London: Institute of Physics) p. 191

173. E. Simoen, C. Clays, V. Privitera, S. Coffa, M. Kokkoris, E. Kosionides, G. Fanourakis, A. N. Larsen, P. Clauws, Nucl. Instrum. Meth. Phys. Res. B **186**, 19 (2002)

174. E. Simoen, C. Clays, A.M. Kraitchinskii, M.M. Kras'ko, V. B. Neimash, L. I. Shpinar, Solid State Phenomena Vols **82-84**, 425 (2002)

175. L. I. Khirunenko, O. A. Kobzar, Yu. V. Pomozov, M. G. Sosnin, and N. A. Tripachko, Semiconductors **37**, 288 (2003)

176. V. V. Emtsev, P. M. Klinger, V. I. Fistful', and Y. V. Shmartsev, Sov. Phys. Semicond. **25**, 602 (1991)

177. R. C. Newman and R. Jones, in Oxygen in Silicon, Semiconductors and Semimetals, edited by F. Shimura (Academic, Orlando, 1994), Vol. 42, p.289

178. C.A. Londos, A. Andrianakis, V.V. Emtsev, G.A. Oganesyan, H. Ohyama, Mater. Sci. Eng. B **154-155**, 133 (2008)

179. H. J. Stain, 2nd Intern. Conf. on Neutron Transmutation Doping in Semiconductors, edit. By J. M. Meese, (Plenum Press, 1979), p. 229

180. C. A. Londos, N. V. Sarlis, and L. G. Fytros, phys. stat. sol. (a) **163**, 325 (1997)

181. A. Chroneos and H. Bracht, Appl. Phys. Rev. **1**, 011301 (2014)

182. C. N. Koumelis, G. E. Zardas, C. A. Londos, and D. K. Leventouri, Acta Crystallogr. A **32**, 306 (1976).

183. J. L. Lindström and B. G. Svensson, Mater. Res. Soc. Symp. Proc. **59**, 45 (1986)

184. E. Hild, P. Gaworzewski, M. Franz, and K. Pressel, Appl. Phys. Lett. **72**, 1362 (1998)

185. Y. V. Pomozov, M. G. Sosnin, L. I. Khirunenko, V. I. Yashnik, N. V. Abrosimov, W. Schröder, and M. Höhne, Semiconductors **34**, 989 (2000)

186. I. Yonenaga, M. Nonaka, and N. Fukata, Physica B **308-310**, 539 (2001)

187. A. Misiuk, J. Bak-Misiuk, A. Barcz, A. Romano-Rodriguez, I. V. Antonova, V. P. Popov, C. A. Londos, and J. Jun, Int. J. Hydrogen Energy **26**, 483 (2001)

188. V. P. Markevich, A. R. Peaker, L. I. Murin, and N. V. Abrosimov, Appl. Phys. Lett. **82**, 2652 (2003)

189. A. V. G. Chizmeshya, M. R. Bauer, and J. Kouvetakis, Chem. Mater. **15**, 2511 (2003)

190. V. P. Markevich, A. R. Peaker, J. Coutinho, R. Jones, V. J. B. Torres, S. Öberg, P. R. Briddon, L. I. Murin, L. Dobaczewski, and N. V. Abrosimov, Phys. Rev. B **69**, 125218 (2004).

191. S. Hao, L. Kantorovich, and G. Davies, Phys. Rev. B **69**, 155204 (2004).

192. A. Chroneos, H. Bracht, R. W. Grimes, and B. P. Uberuaga, Mater. Sci. Eng. B **154-155**, 72 (2008).

193. A. Chroneos, H. Bracht, C. Jiang, B. P. Uberuaga, and R. W. Grimes, Phys. Rev. B **78**, 195201 (2008)

194. A. Chroneos, R. W. Grimes, and H. Bracht, J. Appl. Phys. **105**, 016102 (2009)

195. R. Kube, H. Bracht, A. Chroneos, M. Posselt, and B. Schmidt, J. Appl. Phys. **106**, 063534 (2009)

196. A. Chroneos, C. Jiang, R. W. Grimes, U. Schwingenschlögl, and H. Bracht, Appl. Phys. Lett. **94**, 252104 (2009)

197. A. Chroneos, C. Jiang, R. W. Grimes, U. Schwingenschlögl, and H. Bracht, Appl. Phys. Lett. **95**, 112101 (2009)

198. R. Kube, H. Bracht, J. Lundsgaard Hansen, A. Nylandsted Larsen, E. E. Haller, S. Paul, and W. Lerch, J. Appl. Phys. **107**, 073520 (2010)

199. J. J. Pulikkotil, A. Chroneos, A. Chroneos, and U. Schwingenschlögl, J. Appl. Phys. **110**, 036105 (2011)

200. A. Chroneos, E. N. Sgourou, and C. A. Londos, J. Appl. Phys. **112**, 073706 (2012)

201. H. Tahini, A. Chroneos, R. W. Grimes, U. Schwingenschlögl, and A. Dimoulas, J. Phys. Condens. Matter **24**, 195802 (2012)

202. H. Wang, A. Chroneos, D. Hall, E. N. Sgourou, and U. Schwingenschlögl, J. Mater. Chem A. **1**, 11384 (2013)

203. A. Chroneos, E. N. Sgourou, and C. A. Londos, J. Mater. Sci.: Mater. Electron. **24**, 2772 (2013)

204. E. N. Sgourou, A. Andrianakis, C. A. Londos, and A. Chroneos, J. Appl. Phys. **113**, 113507 (2013)

TABLE 1. Calculated transition levels (in eV) for the *V*O and *V* defects [64].

	*V*O	*V*
(++/0)	-	0.04
(+/0)	-	-
(0/-)	0.54	0.33
(0/--)	0.54	0.27
(-/--)	0.53	0.21
(+/-)	0.11	0.17
(+/--)	0.25	0.18
(++/-)	-	0.14
(++/--)	0.05	0.16

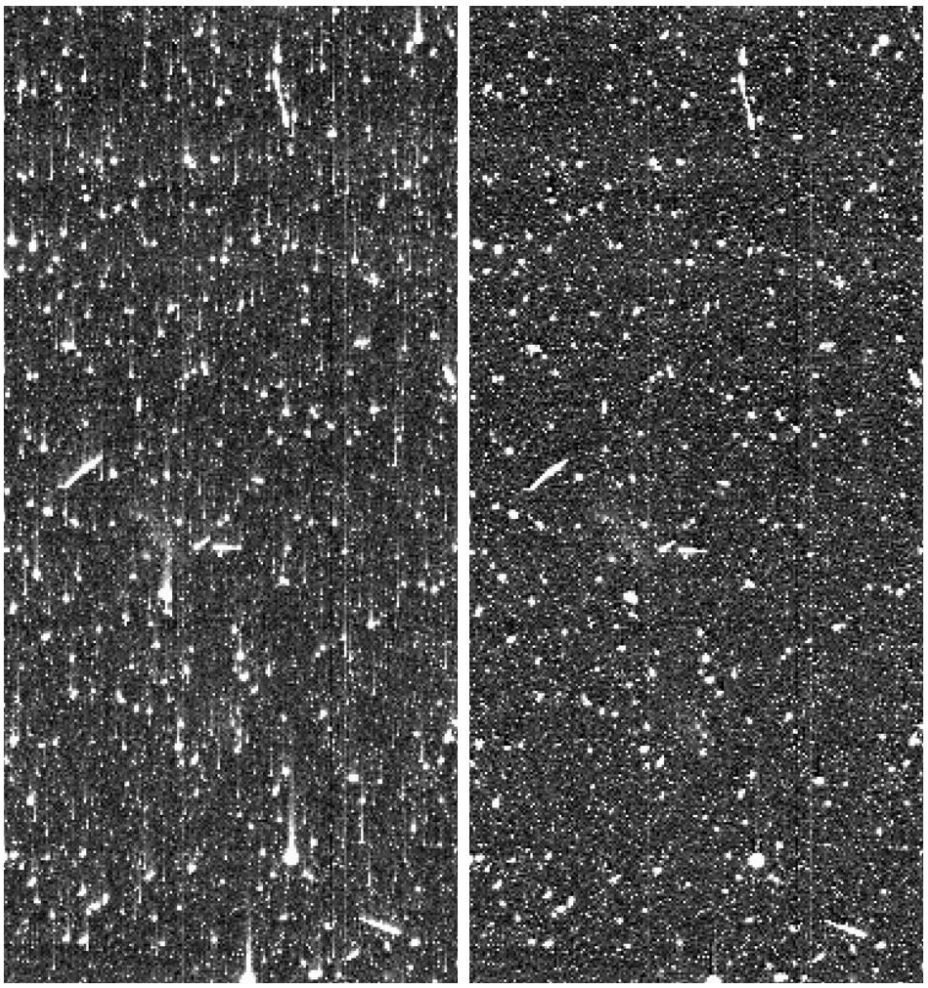

Figure 1. A typical raw ACS/WFC science exposure from early 2010 (HSTGO 11689, PI: Renato Dupke) before (left) and after (right) CTI correction. The 380x820 pixel area selected is furthest on the detector from the readout register, and the logarithmic colour scale is chosen intentionally to highlight the CTI trails [37].

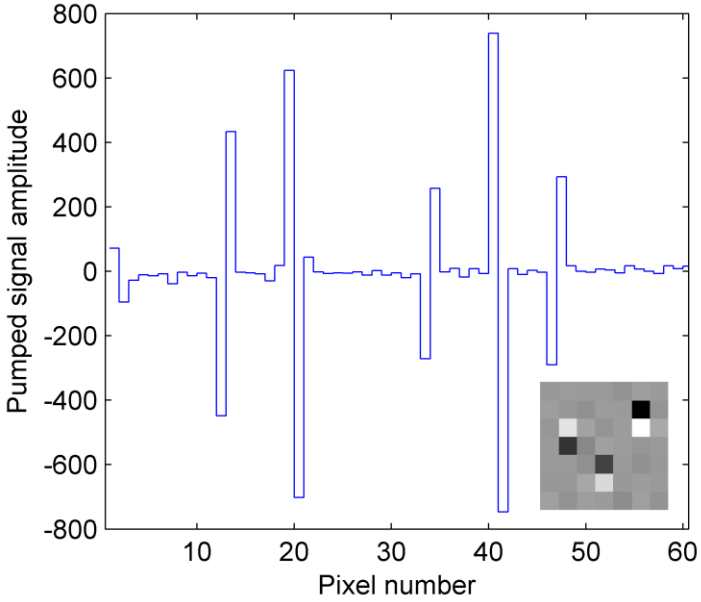

Figure 2. The process of "single trap pumping" allows the study of individual traps in the silicon of a CCD. The image inset shows three black-white dipoles, each one representing the presence of a single trap within the pixel of the CCD. The direction of the dipole (black-white or white-black) is determined by the location of the trap to the sub-pixel accuracy. The line profile shows the presence of 5 traps, each with a different amplitude. The variation in the amplitude with temperature and readout speed allows the determination of individual trap properties [60].

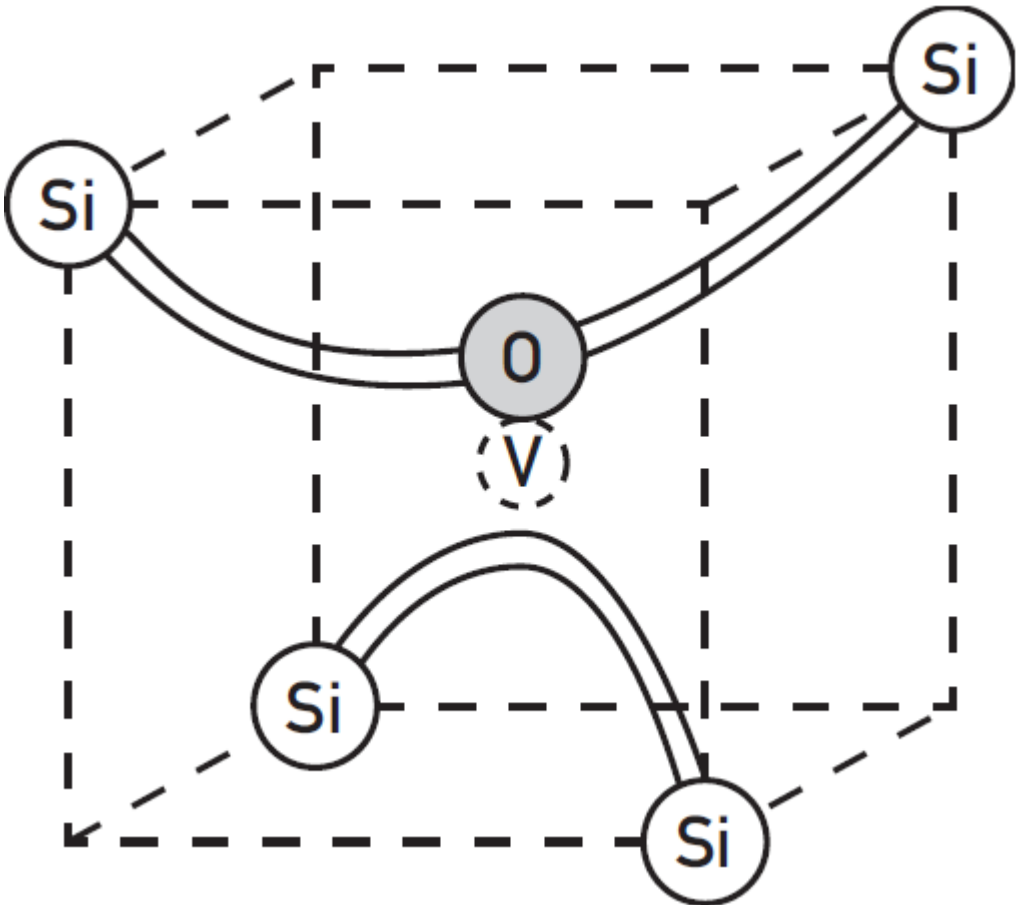

Figure 3. A Schematic representation of the *V*O defect.

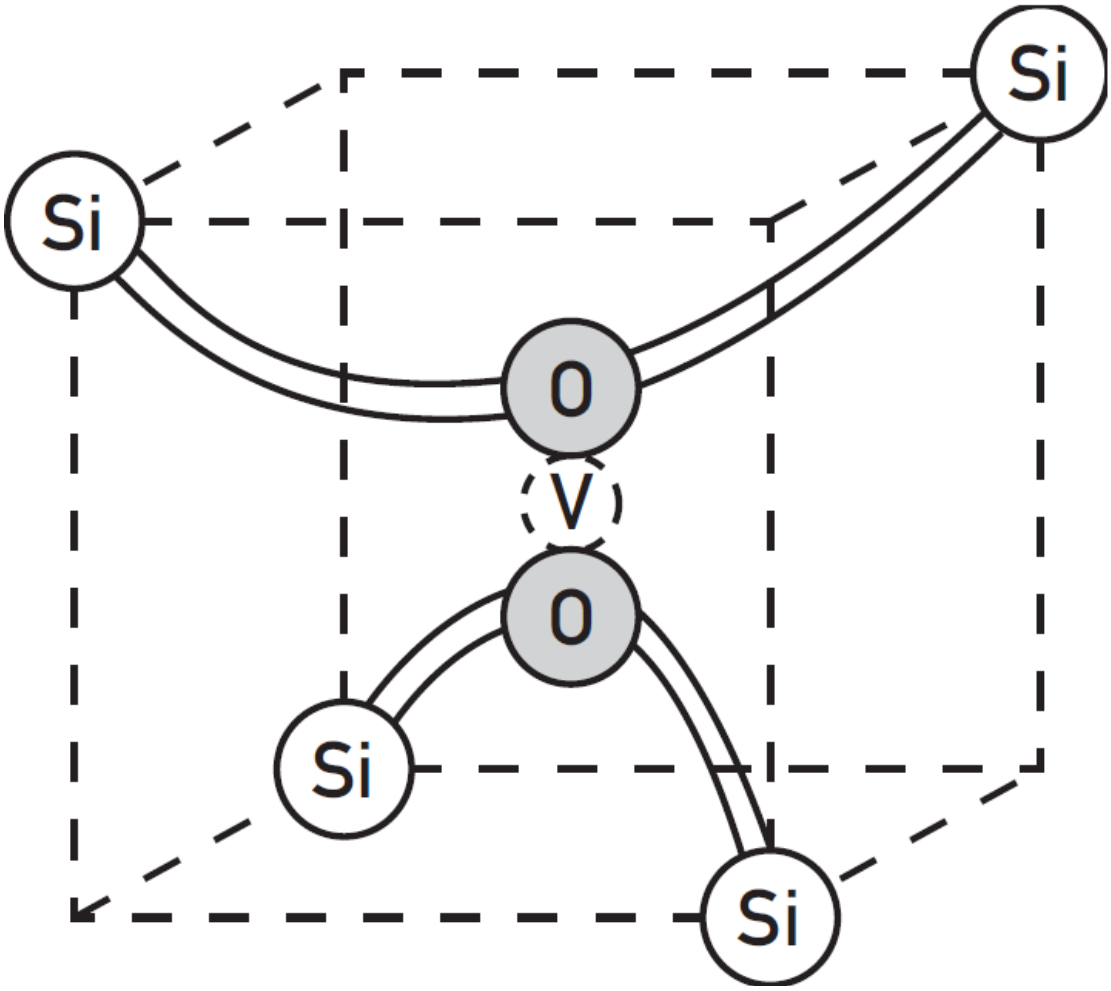

Figure 4. A Schematic representation of the VO_2 defect.

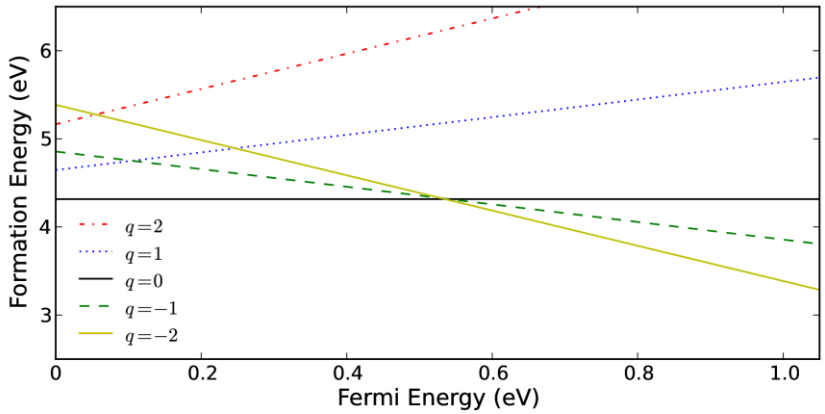

Figure 5. Formation energies of the *V*O defects, with respect to the Fermi energy [54].

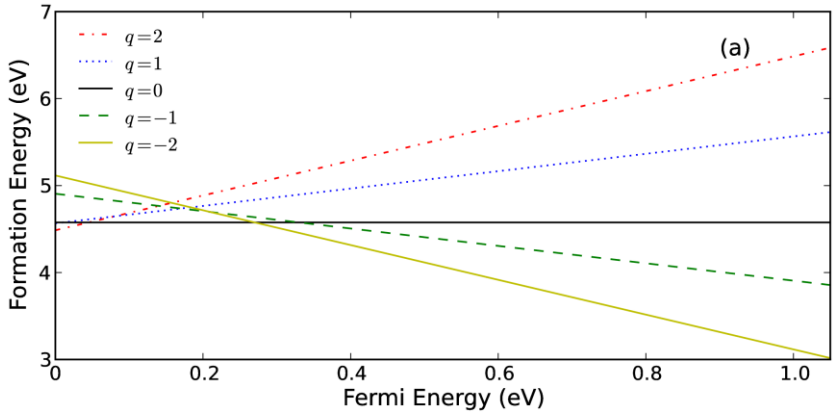

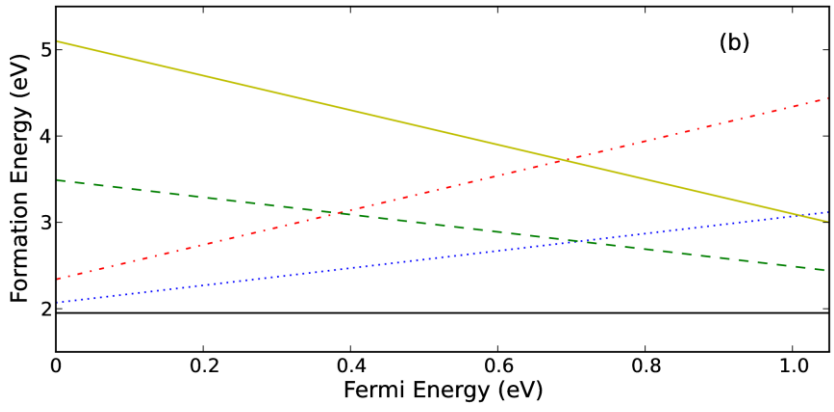

Figure 6. Formation energies of the (a) *V* and (b) O_i defects, with respect to the Fermi energy [64].

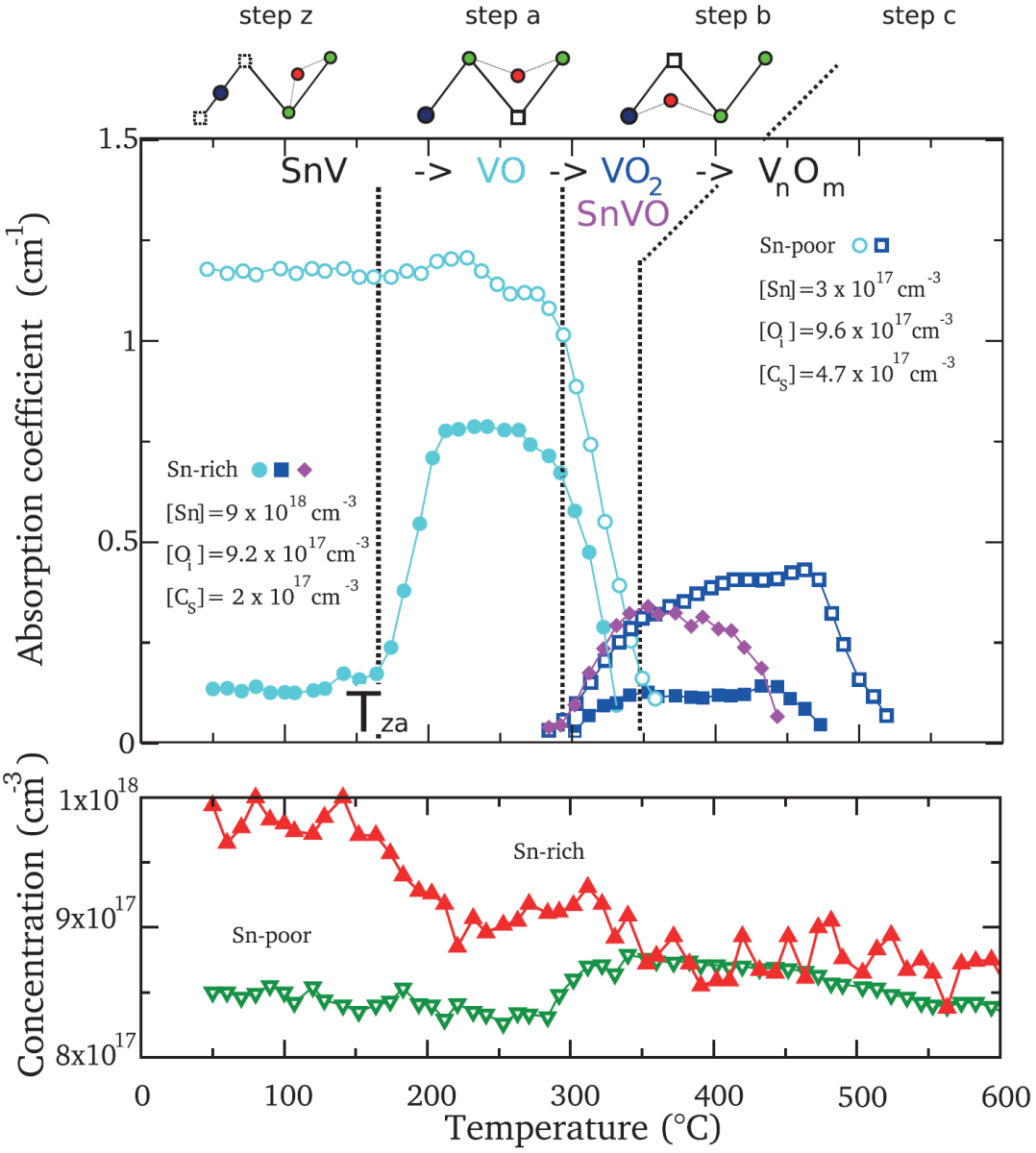

Figure 7. The thermal evolution of *V*O (cyan circles), *V*O_2 (dark blue squares), and Sn*V*O (magenta diamonds) defects for Sn-poor and Sn-rich samples in Si. The upper part represents the defects using blue and green circles for the *D* isovalent atom and Si atoms, square and dotted squares for the *V* and semi-*V*, and red circles for the oxygen atom. The bottom figure represents the thermal evolution of the oxygen interstitials for Sn-poor and Sn-rich conditions [104].

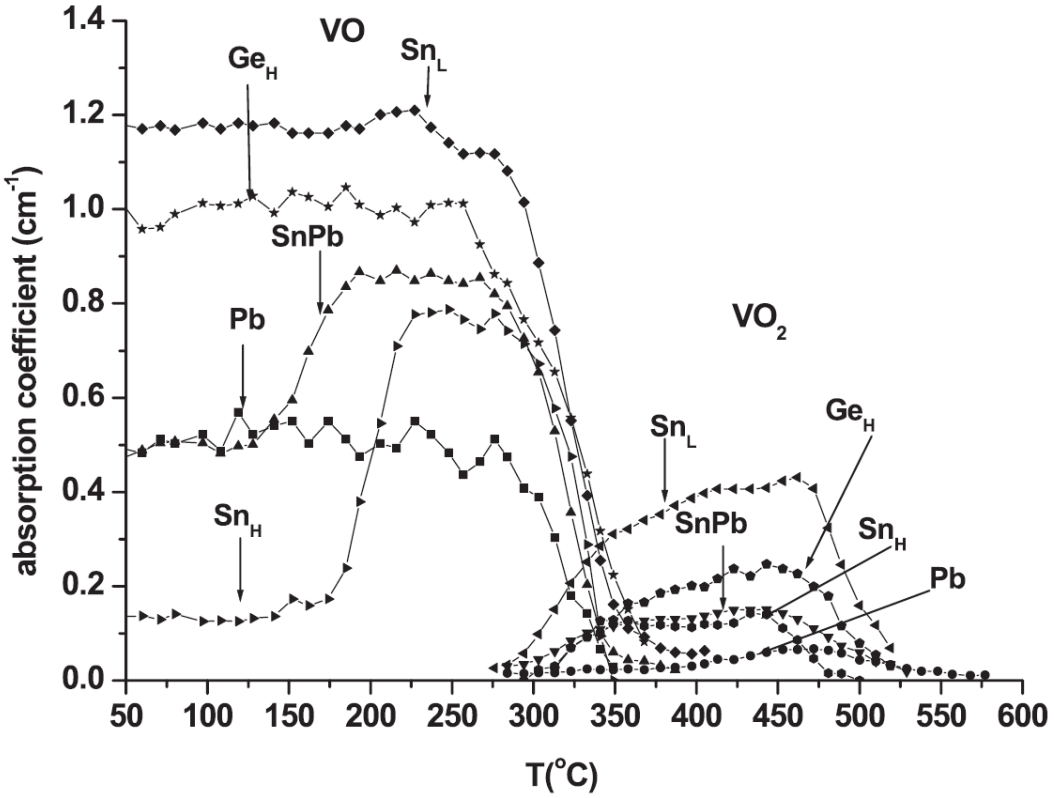

Figure 8. Evolution with respect to temperature of the *V*O and *V*O_2 defects of doped (Ge, Sn and Pb) and codoped (Sn/Pb) Si [98].

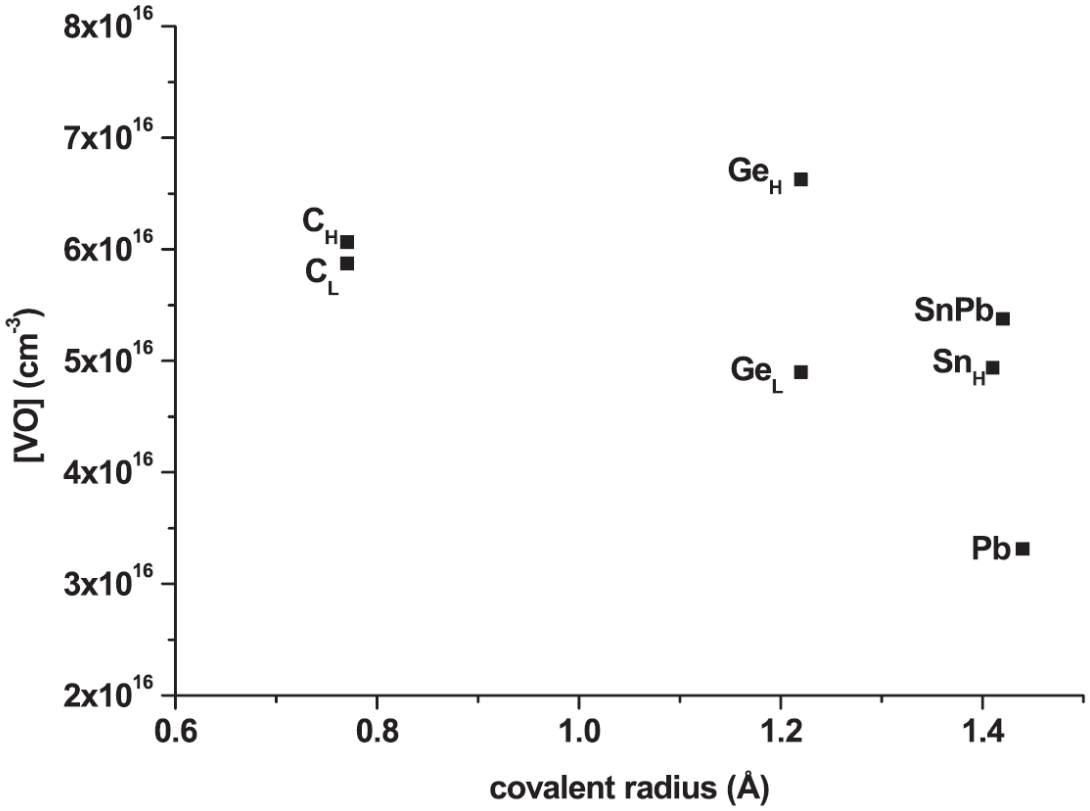

Figure 9. The production of the A-centre with respect to the covalent radius of the isovalent dopants [98].

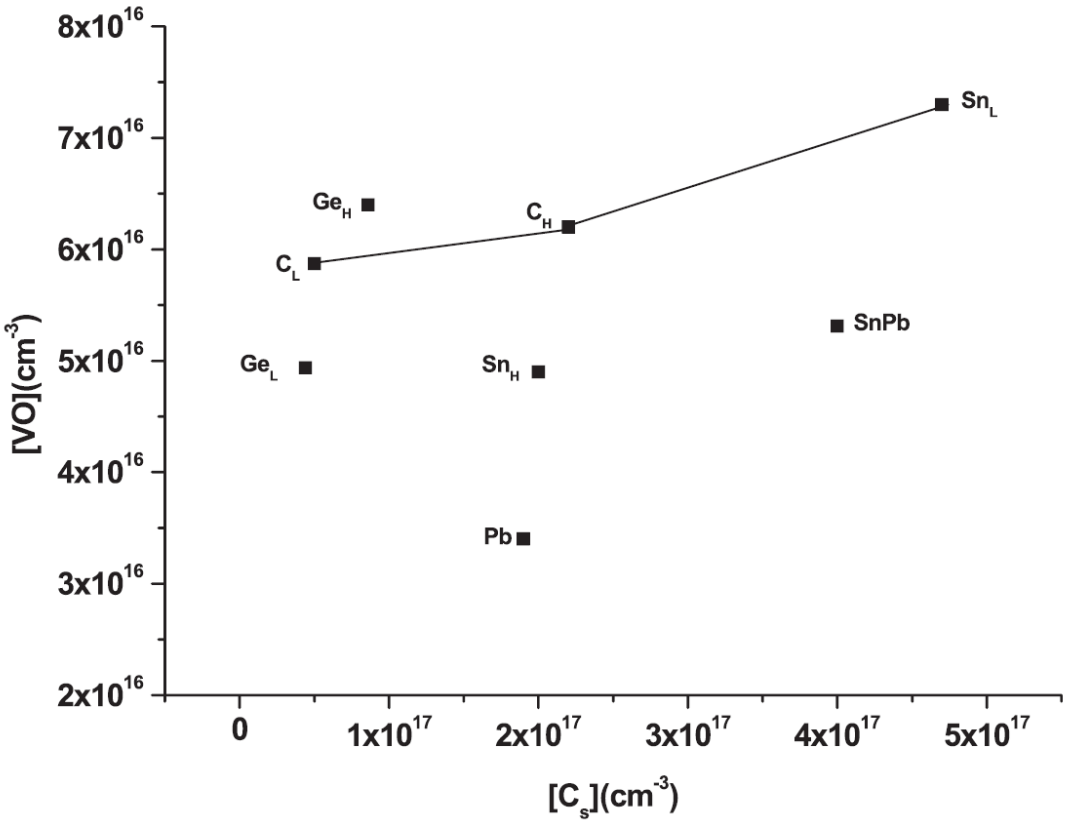

Figure 10. The production of the A-centre with respect to the carbon concentration of of the isovalent doped Si samples [98].

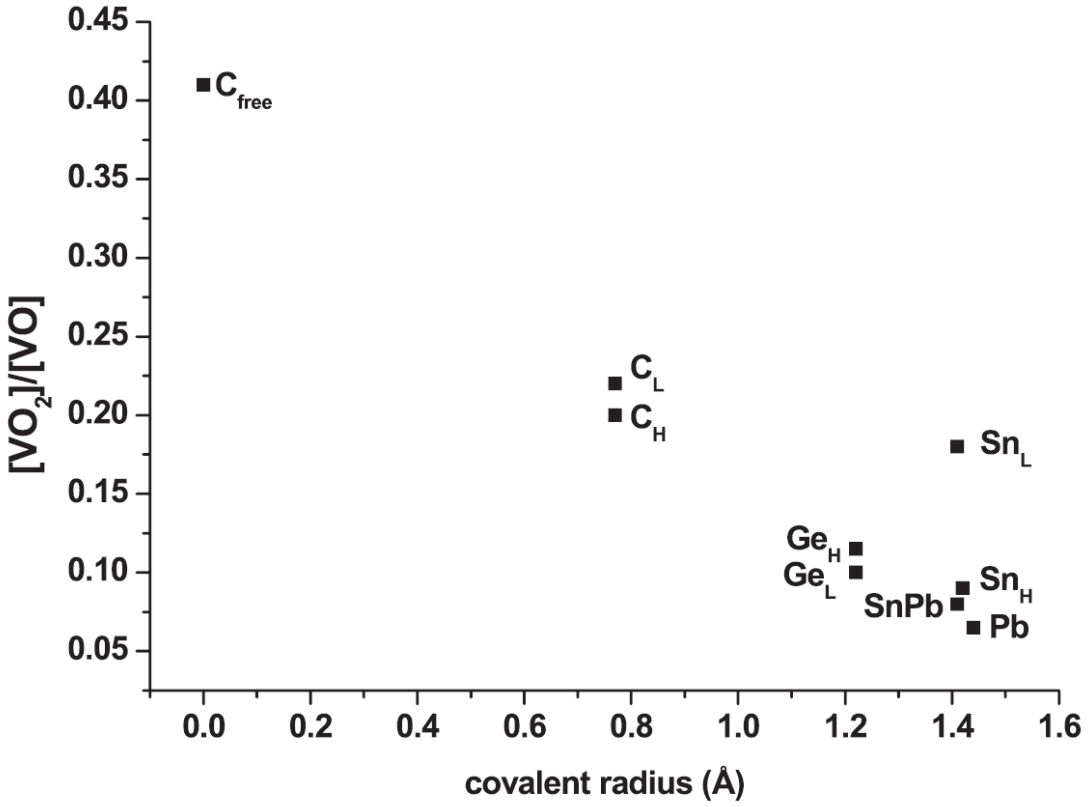

Figure 11. The conversion ratio [VO_2] / [VO] with respect to the isovalent dopant covalent radius in Si [98].

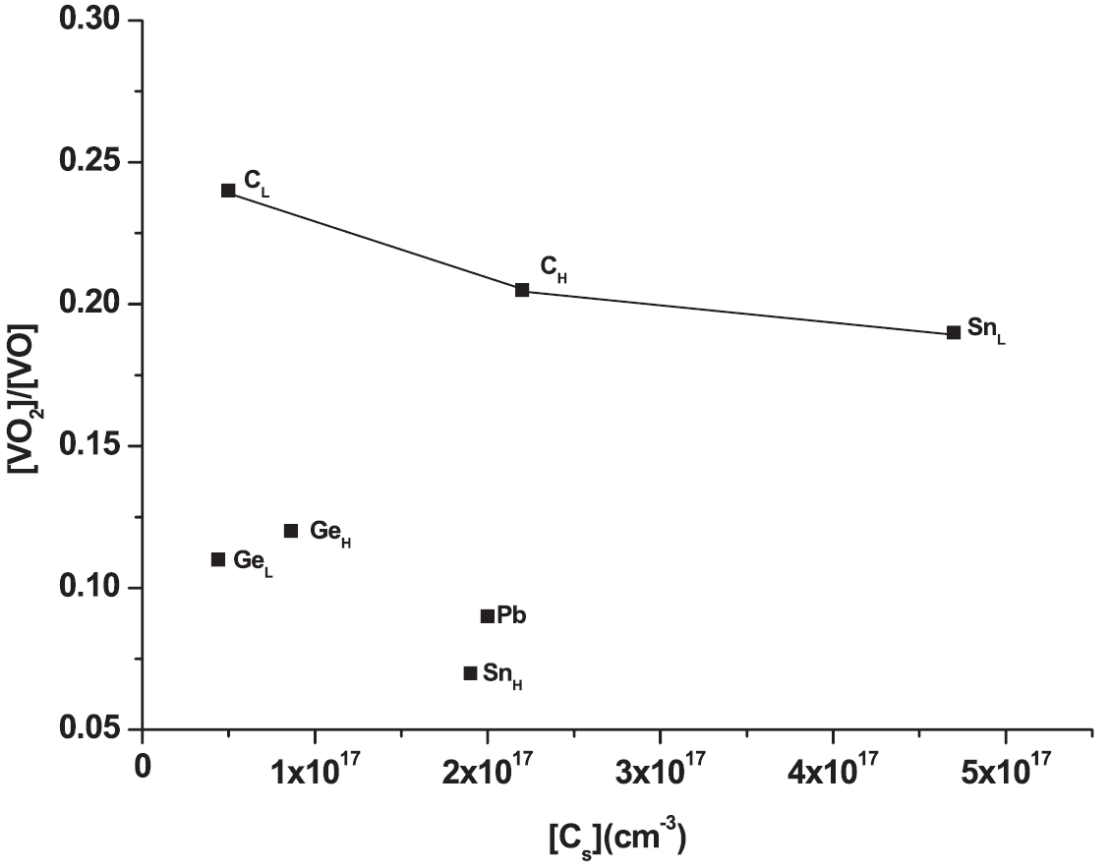

Figure 12. The conversion ratio [VO_2] / [VO] with respect to the carbon concentration of the isovalent doped Si samples [98].

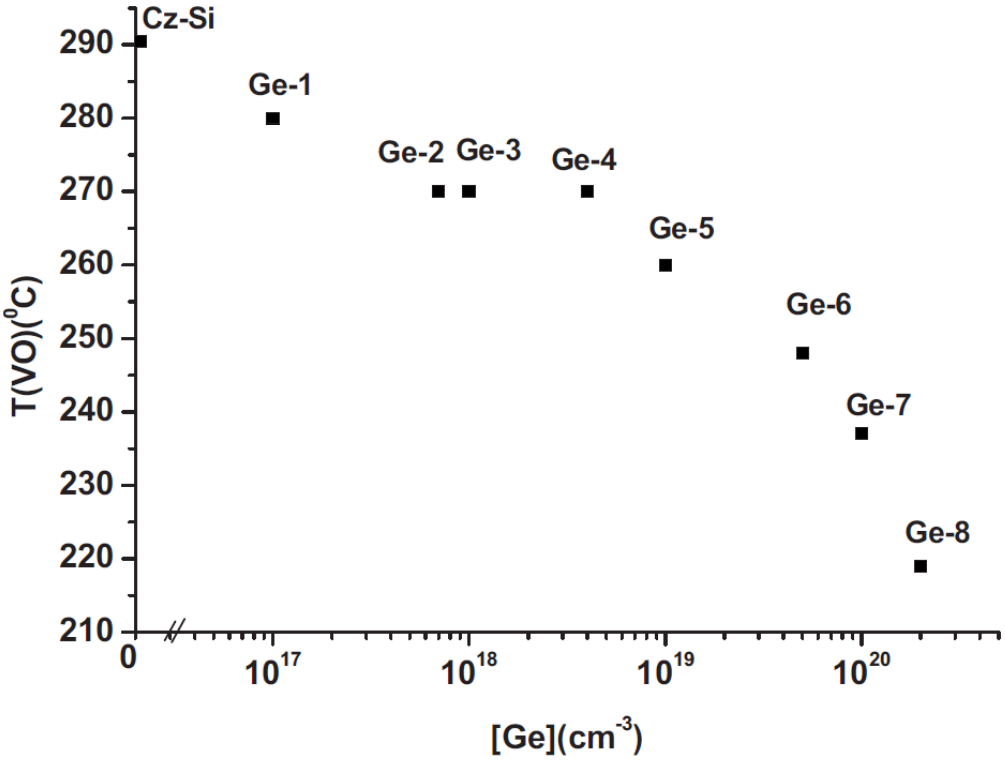
Cz-Si
Ge-1
Ge-2
Ge-3
Ge-4
Ge-5
Ge-6
Ge-7
Ge-8
290
280
270
260
250
240
230
220
210
0
10^{17}
10^{18}
10^{19}
10^{20}
T(VO)(^{0}C)
[Ge](cm^{-3})

(a)

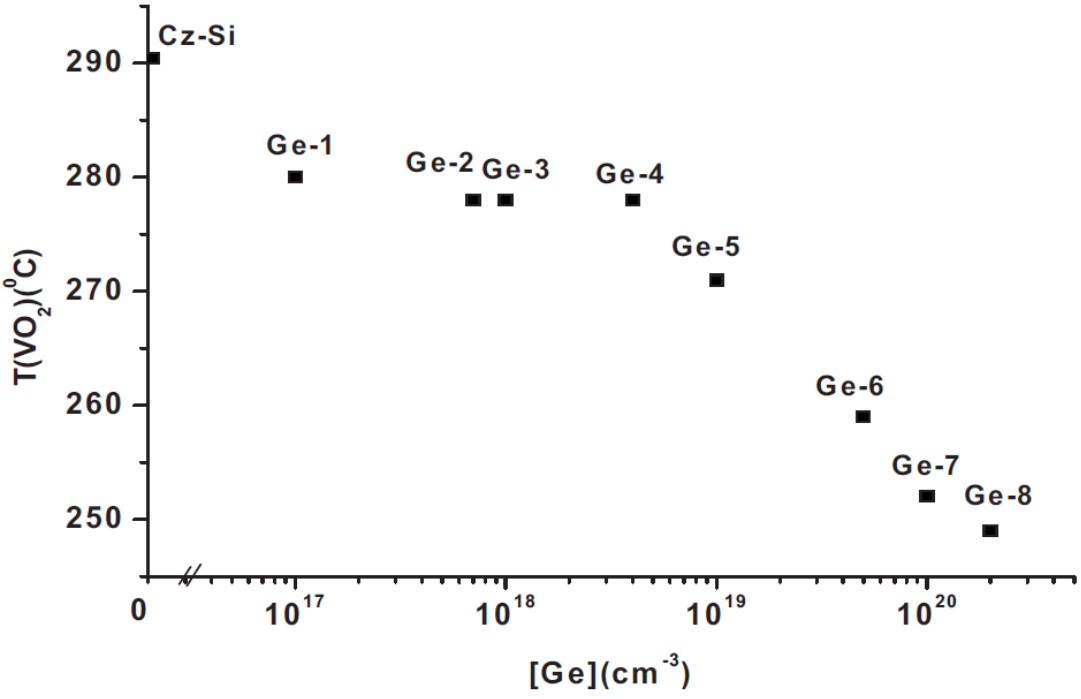
Cz-Si
Ge-1
Ge-2
Ge-3
Ge-4
Ge-5
Ge-6
Ge-7
Ge-8
290
280
270
260
250
0
10^{17}
10^{18}
10^{19}
10^{20}
T(VO$_2$)(^{0}C)
[Ge](cm^{-3})

(b)

Figure 13. (a) Annealing temperature of *V*O defects with respect to the Ge concentration and (b) formation temperature of the VO_2 defects with respect to the Ge concentration [100].